May 2015

A New Correlation for Predicting Aeration Efficiency for Air Diffused Systems

Hasan Baker Mohammad Al Ba'ba'a
University of Wisconsin-Milwaukee

A NEW CORRELATION FOR PREDICTING AERATION EFFICIENCY FOR AIR DIFFUSED SYSTEMS

by

Hasan B. Al Ba'ba'a

A Thesis Submitted in

Partial Fulfillment of the

Requirements for the Degree

Master of Science

in Engineering

at

University of Wisconsin – Milwaukee

May 2015

ABSTRACT
A NEW CORRELATION OF PREDICTING AERATION EFFICIENCY FOR AIR DIFFUSED SYSTEMS

by

Hasan B. Al Ba'ba'a

The University of Wisconsin-Milwaukee, 2015
Under the Supervision of Professor Ryoichi Amano

Aeration efficiency is defined as the ratio of the oxygen transfer to the power consumed. It provides the best evaluation of the effectiveness of any aeration system. Most recent studies in oxygenation process focused on investigating the vital parameters affecting the oxygenation process without paying attention to the power consumption. The goal of this study is to establish an empirical correlation that describes aeration efficiency behavior with different orifice diameters.

This work has two main parts: studying bubble hydrodynamics and aeration efficiency investigation. The first goal of examining bubble hydrodynamics was to calculate some necessary parameters that have a known effect on an aeration process. A second outcome from investigating bubble hydrodynamics was the development of two correlations for predicting bubble size and frequency with correlation factors of 0.95 and 0.92, respectively.

In addition, the dimensionless analysis also was employed to correlate the parameters significantly affecting aeration efficiency. The new developed empirical formula was derived from 120 different experiments with a correlation factor of $R^2 = 0.94$ using SOLVER nonlinear regression in MS EXCEL.

Five parameters were found to be affecting factors on the aeration performance, namely: Gas holdup, static to chamber pressure ratio, submergence height to tank diameter ratio, and aerated to tank area ratio. The parameter with the highest impact was the pressure ratio term, which has the largest power exponent of 0.721.

Future work in this aspect will be implementing optimization techniques to find the best orifice size to be used in manufacturing aeration membranes.

Dedicated to my parents, my most beloved wife, brothers, and sisters
for their love and support.

TABLE OF CONTENTS

LIST OF FIGURES

LIST OF TABLES

LIST OF NOMENCLATURE

a	Elliptical Bubble Major axis (m)
A_a	Aerated Area (m^2)
A_d	Area Covered by Diffusers (m^2)
A_t	Tank Cross-sectional Area (m^2)
b	Elliptical Bubble Minor axis (m)
C	Dissolved Oxygen Concentration at a Certain Time (mg/L)
C_0	Dissolved Oxygen Concentration at time zero (mg/L)
C_∞	Dissolved Oxygen Concentration at saturation (mg/L)
d	Travel Distance (m)
d_b	Sauter Mean bubble Diameter (m)
d_{eq}	Equivalent Bubble Diameter (m)
d_o	Orifice Diameter (m)
D_t	Tank Diameter (m)
$\dot{\mathrm{F}}$	Frame Rate (frame/s)
f_b	Bubble Frequency (Sec^{-1})
Fe	Ending Frame order
Fs	Starting Frame Order
Fr	Tank Froude Number
g	Gravitational acceleration (m/s^2)
h_d	Diffuser Submergence Head (m)

h_t	Tank Height (m)
Kla	Volumetric Mass Transfer Coefficient (hr^{-1})
Kla_{20}	Standard Volumetric Mass Transfer Coefficient (hr^{-1})
Kla_{as}	Volumetric Mass Transfer Coefficient for Activated Sludge (hr^{-1})
Kla_b	Volumetric Mass Transfer Coefficient at Bubble Surface (hr^{-1})
Kla_s	Volumetric Mass Transfer Coefficient at Water Surface (hr^{-1})
N_b	Number of Bubbles
N_T	Transfer Number
p_c	Chamber Pressure (N/m^2)
p_s	Static Pressure (N/m^2)
P	Power (KW)
Q	Standard Gas Volume Flow Rate (m^3/s)
q_m	Gas Mass Flow Rate (Kg/s)
Re	Tank Reynolds Number
Re_o	Orifice Reynolds Number $(= 4q_m/\pi\mu_g d_o)$
SAE	Standard Aeration Efficiency (KgO_2/KWh)
$SOTE$	Standard Oxygen Transfer Efficiency (%)
$SOTR$	Standard Oxygen Transfer Rate (Kg/h)
$SSOTE$	Specific Standard Oxygen Transfer Efficiency (1/m)
t	Time (s)
U_b	Bubble Average Velocity (m/s)
U_g	Gas Superficial Velocity (m/s)

V_b Mean bubble Volume (m^3)

V_w Water Volume (m^3)

We_o Orifice Weber Number ($= 16Q^2\rho_l/\pi^2 d_o^3\sigma$)

$\dot{W}_{O_2}$ Oxygen Mass Transfer Rate (KgO_2/s)

Greek Letters

$\boldsymbol{\alpha}$ Adjustable Dimensional Coefficient

$\boldsymbol{\varepsilon}$ Gas Holdup

$\boldsymbol{\mu_g}$ Gas Kinematic Viscosity $(Pa.s)$

$\boldsymbol{\mu_l}$ Liquid Kinematic Viscosity $(Pa.s)$

$\boldsymbol{\rho_g}$ Gas Density (Kg/m^3)

$\boldsymbol{\rho_l}$ Liquid Density (Kg/m^3)

$\boldsymbol{\sigma}$ Surface Tension (N/m)

$\boldsymbol{\nu_w}$ Water Kinetic Viscosity (m^2/s)

Abbreviations

AE Aeration Efficiency

DO Dissolved Oxygen

SLPM Standard Liter Per Minute

WWTP Wastewater Treatment Plant

ACKNOWLEDGMENTS

Firstly, I would like to express my sincere thanks to my academic advisor Prof. Ryoichi Amano for his support and guidance throughout my whole study. His insights and remarks on my research were very precious and beneficial. This work would not have been possible without his close attention and great support. It was a pleasure to publish this work under his supervision and guidance. Besides my advisor, I would like to thank the rest of my thesis committee: Dr. Emmanuel Wornyoh, Prof. Jin Li, and Dr. Woo-Jin Chang for their encouragement, insightful comments, and constructive criticism.

I would also like to thank my research colleague Dr. Ammar Alkhalidi for his support at early stages of this research. His great experience in wastewater treatment system and aeration process have significantly improved my knowledge in the field.

Great thanks for all of Prof. Amano's research members: Mohamed Ibrahim, Tarek ElGammal, Michael Hamman, Yi-Hsin Yen and Alka Gupta for their support and suggestions to help me improve my research skills.

No words can express how thankful I am for my father Baker Al Ba'ba'a and my mother Sabah Al Shareef, who worked day and night to make me reach this stage of my life. I hope with this achievement that I reciprocate a little from what they provided me.

Chapter 1: Introduction to Wastewater Treatment

Wastewater is any water that has been affected by anthropogenic influence. On a daily basis, water is polluted by the industrial facilities byproducts, ground infiltration, storm water and municipal discharges, from which the wastewater is generated (Davis, 2010). Although nature plays a remarkable role in treating a small amount of water contaminants, billions of gallons of wastewater and sewage produced every day cannot be treated naturally. Hence, the presence of wastewater treatment plant (WWTP) is essential to ensure remediation of pollutants before releasing water back to the environment. Failure of treating wastewater results in a potential detriment to human and ecosystem. Discharging wastewater to the environment without remediation causes generation of foul gases in large quantities. In addition, it elevates the chance of spreading diseases because of the pathogenic microbes and poisonous compounds (Metcalf and Eddy, Inc., 1979).

1.1. Wastewater Treatment Stages

The wastewater treatment is defined as the process through which impurities and organic substances are removed. Wastewater goes through three main remediation stages, named: Primary, Secondary and Tertiary. A preliminary treatment is applied to reduce the need for maintenance due to problems may happen during the treatment process. Through this preliminary process, a considerable amount of large solids, grit and untreatable materials is removed prior subjecting wastewater to the core remediation processes (EPA, 2004). Screens, shredders or grinders and flow equalization are examples

of operations used in a typical preliminary treatment process. (Davis, 2010). Figure 1-1 below shows a schematic diagram for such a treatment plant with two equalization designs: Online and Offline equalization.

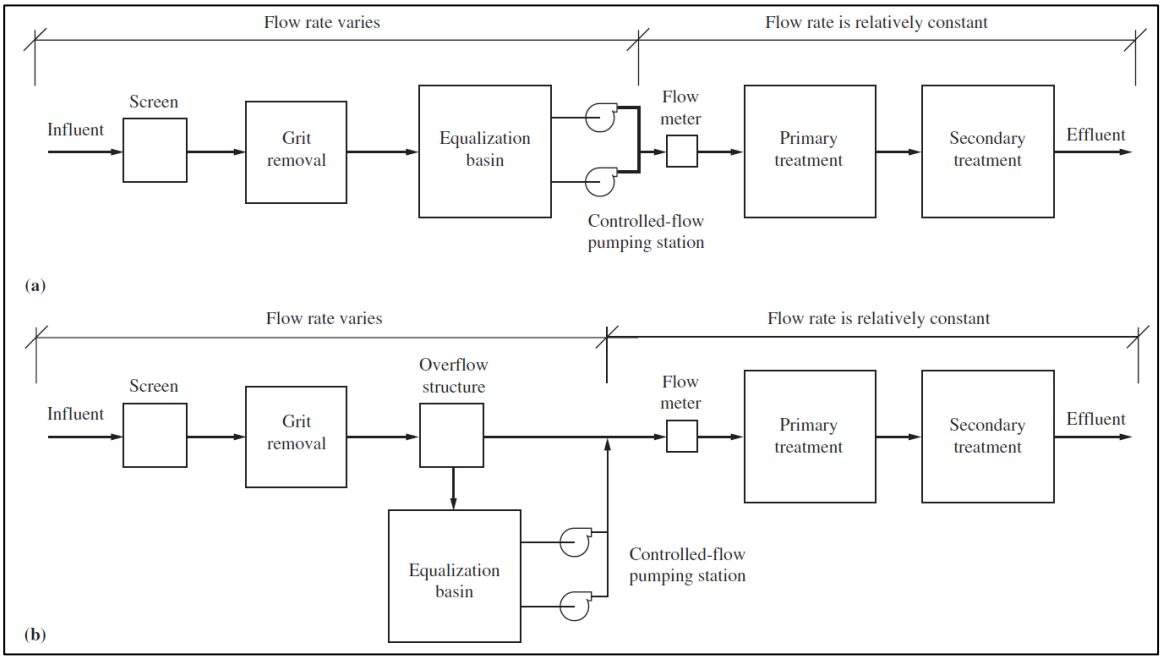

Figure 1-1: Schematic diagram for a wastewater treatment plant: (A) Inline Equalization and (B) Offline Equalization (Davis, 2010).

1.1.1. Primary Treatment

Primary treatment is the first stage of the remediation process. After the influent wastewater is cleared from large solids and grit, a significant portion of the organic matter is removed by means of sedimentation, the main method of primary treatment. Sedimentation is achieved by holding water in a large tank for a sufficient time to allow heavy solids to settle to the bottom while light and floatable matter rise to the top. This process of removing sediment solids and floating matter saves a significant amount of energy because of the declination in BOD_5 value. In addition, it reduces the chances of

any potential problem that may occur in the downstream biological treatment. (Davis, 2010)

1.1.2. Secondary Treatment

Aerobic biological treatment is the fundamental process of the secondary treatment. After removing around 60% of suspended solids in the primary stage, wastewater is conveyed to an aeration basin where aerobic biological treatment occurs. At the aeration basin, air is continuously supplied to the water to maintain a suitable environment for microorganisms to digest organic matter. During this process, the biodegradable matter is oxidized into Carbon Dioxide and water. In addition, a further remediation of suspended solids escaped from the primary stage is performed. Typically, the duration of an aerobic treatment is approximately six to eight operational hours (Davis, 2010). The effluent of aerobic treatment has excellent quality in comparison to natural treatment of biological waste due to its greater treating capacity (EPA, 2000). Eventually, the treated water may be discharged to the nearest stream, or subjected to a final treatment process.

1.1.2.1. Aeration Process

As highlighted in the previous section, aeration is a process through which air is added to water. Two basic types of aerators are mainly used in WWTPs: mechanical and subsurface aerators. Mechanical aerators uses blades or brushes to shear wastewater surface into small droplets that splash into the atmospheric air to allow oxygen transfer. On the other hand, subsurface aerators (or diffused aeration systems) diffuses air from the bottom of the aeration basin using devices that are diverse in shapes and dimensions

(EPA, 1999). These aeration devices are classified into fine or coarse diffusers depending on their physical properties rather than the size of bubble generated. The reason for adopting physical properties as a classification method is the complexity of identifying a transition line between fine and coarse bubble (Solomon, Casey, Mackne, & Lake, 1998). Examples of fine bubble aerators are plates, discs, tubes and domes; whereas fixed orifices, valve orifices and static tubes are types of coarse bubble aerators.

The primary mechanism behind aeration is the mass transfer between air and water. The two-film theory developed by Lewis and Whitman (1924) provides the best explanation for the gas transfer to a particular liquid. The theory states that the boundary (or the interface) of gas-liquid phases is two distinct films. These films function as barriers between gas and liquid bulks. To dissolve a gas molecule in a liquid, the gas molecule has to pass through four distinct regions: gas bulk, gas film, liquid film and eventually liquid bulk, where a gas molecule diffuses. The reversed path applies for a gas molecule leaving the liquid. Figure 1-2 shows an illustrative diagram for the two-film theory.

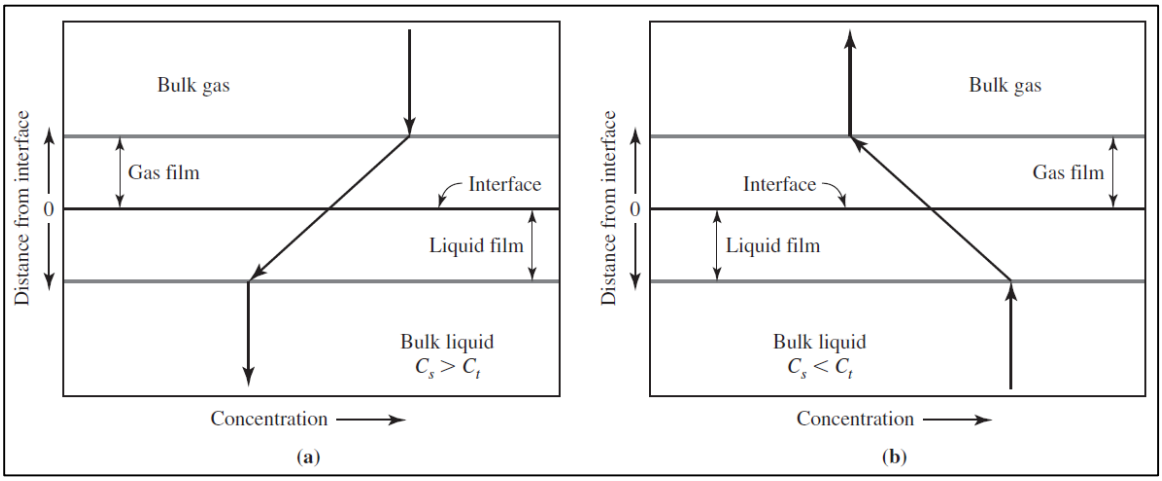

Figure 1-2: Thet wo-film theory model: (a) absorption mode (b) desorption mode (Davis, 2010).

1.2. Problem Statement

Aeration is an energy demanding process. Typically, 50 to 65% of the total remediation cost of wastewater treatment plant is consumed by an aeration process (EPA, 1999). This percentage may vary between 30 to 75% of total power demand depending on the dimensions and operations of a WWTP. Having a wide-ranging geometrical and operational characteristics gives researchers the opportunity to explore and advance aeration devices (Pittoors, Guo, & Van Hulle, 2014b). The interest in investigating fine diffusion systems started following the energy crisis in 1970s by virtue of its power saving (EPA, 1999). Approximately, a 50% reduction in energy depletion can be achieved by replacing coarse bubble diffusers with a fine air-diffusion system (Stenstorm & Vazirinejad, 1984). Since that time, fine bubble diffusers have gained more attention from researchers to develop a highly- efficient aeration systems.

1.3. Research Motivation

Besides providing the required oxygen for microorganisms to proliferate and digest organic materials, aeration offers gentle mixing for microorganisms to be in continuous contact with organic matter (EPA, 1999). Despite being considered the most expensive part of the treatment process, aeration is essential to provide microorganisms which treat organic impurities, with ample amount of oxygen for their nourishment. Adequate air flow must be provided to the aeration basin to prevent any potential problems resulting from an oxygen-poor environment (Pittoors, Guo, & Van Hulle, 2014b).

The effectiveness of an aeration system is represented by a parameter called aeration efficiency (AE) or energy efficiency, which is the actual amount of oxygen transferred to

water per unit of power consumption (KgO_2/KWh). The term efficiency might be misleading as aeration efficiency has a dimensional unit. Efficiency is commenly a dimensionless number that represents the ratio of output to input, where both have the same unit. This represents the amount of utilization of the original input. However, the case of aeration efficiency is different; its input (Electricity) has a different unit from its output (Oxygen Mass Transfer). Therefore, it is reasonable to name this term aeration efficiency since it agrees with the general efficiency definition: the ratio of output to input.

Improving oxygen transfer rate (OTR) and reducing the aeration membrane backpressure are the main techniques for achieving a cost-effective aeration system. Despite improving OTR being essential to an aeration system, it does not necessarily mean a higher AE. A substantial factor affecting AE is the amount of backpressure developed underneath the aeration diffuser even if a higher OTR is obtained. Nevertheless, OTR should be taken into consideration especially when the amount power consumption is maintained.

Through this research, several experimental investigations were performed to better understand and predict AE. These studies can be summarized as: (1) establishing an empirical model for AE prediction and (2) figuring out the orifice size at which the highest AE possible can be achieved.

1.4. Thesis Outline

This study is divided into six chapters in addition to the appendices for the calculation details and raw data that were collected throughout this study.

Chapter one describes waste water treatment and its stages, aeration process, mass transfer concept, problem realization, and research motivations.

Chapter two reviews previous literature on the topics of: Oxygen mass transfer process and its affecting parameters, volumetric mass transfer coefficient prediction and bubble formation correlations.

Chapter three provides in detail description of the experimental setups used in this study, the methods of approach and data analysis.

Chapter four and five present the experimental results for both bubble size and frequency correlation and AE Empirical formula, respectively.

Chapter six concludes this study with some inferences and notes that may help improve research in this field in the future.

Chapter 2: Literature Survey

Mass transfer in the gas-liquid interface is widely investigated in literature. The vast diversity in systems including gas-liquid flow makes the factors that affect mass transfer enormous in number and various in significance. Besides studying the effect of certain parameters on the mass transfer performance in gas-liquid interface, further studies have been conducted to develop mathematical models and empirical correlations for such complex flows. These models and correlations have been established to predict the mass transfer coefficient for either specific or general situations. This literature review briefly summarizes some of the experimental and theoretical work that investigated the affecting parameters and mass transfer prediction of the air-water interface.

2.1. Factors Affecting Oxygen Transfer

Ashley *et al.* (1990) conducted an experimental study to investigate the effect of surface condition and orifice diameter using a 239 L lab scale aeration tank. The four standard parameters assessing oxygen transfer process (KLa, SOTR, SOTE and SAE) were studied. Under 28.3 LPM air flow rate, the oxygenation performance was tested for one fine air diffuser with a maximum pore diameter of 40 µm and two coarse air spargers with an orifice diameters of 397 and 1588 µm. All of which were tested under three different surface conditions: covered, uncovered, and uncovered with induced wind. For the latter condition, an air blower was employed to generate 0.5 – 1.0 cm waves on the water surface. The coarse air diffusers (397 and 1588 µm) were implemented using four PVC pipes. To maintain the constant perforated area, four orifices were drilled (one orifice per

pipe) for the 1588 µm sparger while 397 µm sparger had a total of 64 orifices (16 orifices per pipe). For the 40 µm fine air diffuser, model (AS-8-0) aerator from Aquatic Eco-Systems, Inc. was acquired. Results showed that smaller orifice diameter enhanced all parameters mentioned above (KLa, SOTR, SOTE and SAE) considerably. The 397 µm and 40 µm orifice sizes showed twice and thrice the efficiency of the 1588 µm one respectively. The fine air diffuser was the most efficient among the three diffusers, and the surface condition had no significant contribution in enhancing oxygen transfer regardless of perforate diameter.

To further their studies in factors affecting oxygen transfer, Ashley *et al.* (2009) conducted another experimental study using a pilot scale full lift hypo limnetic aerator. This study aimed mainly to examine the effect of submergence depth, airflow rate and perforate size on the oxygen transfer process. At an airflow rate of 10, 20, 30 and 40 LPM, the authors tested the aerator's performance under two different diffuser depths (1.5 and 2.9 m) with three orifice sizes (140, 400 and 800 um). These tests were repeated three times as recommended by ASCE (1993) to be a total of 72 experiments. At all testing flow rates, the study concluded that increasing diffuser depth and decreasing orifice size enhanced all KLa, SOTR, SOTE and SAE; whereas elevating air flow rate negatively impacted SOTE and SAE only. For higher water depth, an improvement ranging from 30 to 57% was achieved because of the longer contact time and the higher concentration gradient. This SAE enhancement was unexpected as a similar study in literature showed opposite results (Mavinic & Bewtra, 1976). The authors attributed this discrepancy to the additional power consumption required for water pumping in Mavinic and Bewtra's

study. As smaller orifice generates finer air bubbles, which is the second factor studied, the oxygenation performance was greatly improved due to greater interfacial area per unit volume and longer contact time (resulted from lower terminal velocity). Finally, the rising in power demand associated with elevated airflow rates resulted in the decayed performance of SAE, while larger air bubble generated at higher airflow rate was the cause of SOTE decline.

2.2. Oxygen Transfer Prediction

Painmanakul *et al.* (2009) suggested a new theoretical prediction method for the volumetric mass transfer coefficient (KLa) in gas-liquid flow based on the separation of the mass transfer of the liquid side (KL) and the interfacial area (a). The proposed technique considered the bubble diameter as the primary parameter from which other bubble characteristics like bubble surface area, frequency and rising velocity were determined. These characteristics were then used to estimate the interfacial area (a) of the generated bubbles as well as (KL). Finally, KLa was determined by simply multiplying (a) and (KL). All these bubble characteristics, including bubble diameter and liquid mass transfer coefficient (KL), were calculated using correlations that the authors acquired from literature. Under operating conditions of Reynolds number of 150-1000 and Weber number of 0.002-4, the authors experimentally compared their results using a small laboratory scale bubble column. The experiments were done by injecting gas through an elastic membrane with a single orifice into tap water. The study showed that, regardless the operating conditions, the bubble size, frequency and rising velocity were found to be the main parameters that can predict both KLa and KL.

Gillot *et al.* (2005) studied the influence of some geometrical and hydrodynamic parameters of aeration tanks on the oxygenation process experimentally. A total of 21 measurements of oxygenation were conducted from 12 real aeration tanks that varied in depth (2.4 to 6.1 m). Using dimensional analysis, the authors established equation (2-1) that provides an accurate prediction of oxygenation performance in aeration tanks. The dimensionless relationship was based on the transfer number equation generated by Capela (1999) that was a function of the oxygen transfer coefficient. Furthermore, two relationships were established to estimate the mass transfer coefficient and the specific standard oxygen transfer efficiency (SSOTE). Equations (2-1), (2-2) and (2-3) below show the developed relationships of transfer number, mass transfer coefficient and the specific standard oxygen transfer efficiency respectively.

$$N_T = \frac{KLa_{20}}{U_G}\left(\frac{\nu^2}{g}\right) = 7.77 \times 10^{-5}\left(\frac{A_d}{A_t}\right)^{0.24}\left(\frac{A_d}{A_a}\right)^{-0.15}\left(\frac{D_t}{h_d}\right)^{0.13} \quad (2\text{-}1)$$

$$KLa_{20} = 1.69QA_t{}^{-1.18}A_d^{0.10}A_a^{0.15}h_d^{-0.13} \quad (2\text{-}2)$$

$$SSOTE = 5.27A_t{}^{-1.18}A_d^{0.10}A_a^{0.15} \quad (2\text{-}3)$$

Concluding their study, the air flow rate (Q_G), diffuser submergence (h), surface area of the tank (S), surface area of diffusers (S_d) and the aerated area (S_a) were found to be affecting factors on the oxygenation process in fine air-diffused aeration tank. For the same water height, oxygen transfer enhanced with the increase in both diffuser number and aerated area when a constant diffuser number was applied. Moreover, the submergence depth and air flow rate did not show any significant influence on the SSOTE.

Based on 179 aeration tests, Schireholz *et al.* (2006) established two empirical equations that predict the surface volumetric mass transfer coefficient, KLa_s, and the bubble mass transfer coefficient, Kla_b (See Equations 2-4 and 2-5). Their data have been obtained from different tank sizes with an air injection depth ranging from 2.25 to 32 m. In addition, tests were conducted in four different sites as follow: LACSD, Sanitaire, WES and Lower Grainte Lock. The calculations of KLa_s and KLa_b were acquired from the mass transfer model by DeMoyer *et al.* (2003).

It was concluded that increasing flow rate had a positive effect on Kla_b while increasing water volume depressed Kla_b value. In addition, the correlation showed that increasing air flow rate and water depth increased KLa_s linearly and to the power of 0.28, respectively. The performance of air-diffused systems were found to be predicted more accurately when the mass transfer coefficient for bubble and surface was calculated separately. Furthermore, the fine bubble diffuser system was found to be 6 times as efficient as the coarse bubble system in terms of Kla_b.

$$\frac{KLa_s}{Q_a} = 49\left(\frac{D}{\nu}\right)^{1/2}\left(\frac{h_d^2}{A_t}\right)^{0.28} \quad (2\text{-}4)$$

$$KLa_b = \alpha\left(\frac{D}{\nu}\right)^{1/2}\left(\frac{Q}{A_t}\right)^{6/5} h_d^{1/10} \quad (2\text{-}5)$$

Relationships for assessing oxygen transfer coefficient have been established by several studies before. However, the impact of activated sludge processes (ASPs) in biological wastewater treatment process is usually not considered, as indicated by Pittoors *et al.* (2014a). This parameter is vital and should be considered in studying biological treatment. To overcome this deficiency, Pittoors *et al.* (2014a) have conducted a bench-

scale experimental study to establish relationships that have better assessment of oxygenation process for non-reactive and ASPs conditions. These equations can be further utilized for larger full scale facilities with acceptable tolerance. The study provided two empirical formulas, correlating twelve essential parameters in wastewater treatment. The air flow rate, diffuser depth and bubble size had the most significant impact on oxygen transfer coefficient in both cases (non-reactive and ASPs). Moreover, air flow rate had the highest influence followed by submergence depth and bubble size.

$$\frac{D_t^2 KLa}{D} = 0.030\, Re^{1.718} Fr^{-0.79} \left(\frac{d_b}{h_d}\right)^{-0.291} \left(\frac{h_t}{D_t}\right)^{-0.554} \left(\frac{A_d}{A_t}\right)^{0.135} \left(\frac{D_t}{h_d}\right)^{0.321} \left(\frac{h_t}{h_d}\right)^{0.086} \left(\frac{V_w}{A_d^{1.5}}\right)^{-0.017} \quad (2\text{-}6)$$

$$\frac{D_t^2 KLa_{AS}}{D} = 0.060\, Re^{1.906} Fr^{-0.631} \left(\frac{d_b}{h_d}\right)^{-0.23} \left(\frac{h_t}{D_t}\right)^{-0.120} \left(\frac{A_d}{A_t}\right)^{0.326} \left(\frac{D_t}{h_d}\right)^{0.164} \left(\frac{h_t}{h_d}\right)^{0.173} \left(\frac{V_w}{A_d^{1.5}}\right)^{-0.01} \quad (2\text{-}7)$$

The behavior in the presence of biomass was slightly different (with a variation of 66% in coefficients at max) as it can be inferred from equations 2-6 and 2-7. Besides this variation, the diffuser surface area was found to be an extra important factor that improved the oxygenation process in the ASPs case as it enhanced liquor mixing and bubble dispersal.

2.3. Bubble Formation

An experimental study was done by Gnyloskurenko *et al*. (2003) to investigate the surface phenomenon effect on bubble creation from a 1-mm single orifice submersed in water at relatively low air flow rate (around 2 cm^3/min) within a contact angle range of $68^o \leq \theta \leq 110^o$. The authors studied bubble generation by monitoring several parameters: surface area, bubble volume, radius at the tip and bubble dimension at the interface.

Bubble formation stages were classified as: nucleation, under critical growth, significant growth, and necking. The study found that bubble size depends mainly on wettability which means that bubble size dramatically increases as contact angle increases.

Leibson *et al*. (1958) observed the air bubble formation mechanism in water on a shape-edge orifice ranging from 0.0165 to 0.1265 inch in diameter with a Reynolds number in the range of $200 < Re_o < 10000$. The outcome of their research was two correlations that describe bubble mean diameter for both laminar and turbulent regions, where critical orifice Reynolds number was 2100. Orifice size is known to have a significant influence on bubble formation at Reynolds numbers less than 2100, but becomes a function of gas flow rate only at higher orifice Reynolds number.

Further investigation was conducted by Kumar *et al*. (1976) since most developed formulas are unpredictable especially at high values of Reynolds numbers. Consequently, the authors investigated air bubble generation to cover deficiencies seen in most of the previous work; like in Leibson *et al*. (1958) and Van Krevelen and Hoftijzer (1950). Kumar *et al*. (1976) investigated three distinct ranges of orifice Reynolds number to successfully establish a correlation that describes each of them. By using the chemical area method, air bubble diameter was detected in three liquid mediums, namely: water, Glycerol (40%) and Kerosene.

In contrast to previous literature discussed above, Wilkinson *et al*. (1994) studied the bubble size in pressurized bubble columns in three different liquids, namely: Mono-ethylene Glycol, N-heptane and Sodium Sulphite water, with pressure between 0.1 and 1.5 MPa, and superficial velocity between 0.02 and 0.1 m/s. Nitrogen was mainly used as

the gas phase for most cases except for deionized water where Helium, Argon, Carbon Dioxide and Sulphur Hexafluoride were also tested. Using the photographic technique, bubbles were captured and analyzed to correlate the vital parameters affecting bubbles along with using data from literature. It was found that bubble size, in this case, was smaller due to higher gas density.

Kantarci *et al.* (2005) reviewed the correlations developed to predict bubble size generated from a single orifice (Table 2-1); in addition to correlations summarized by Painmanakul *et al*. (2009).

Table 2-1 Summary of correlations for bubble size.

Correlation	Conditions	Researcher	Reference
$d_b = 0.18 d_o^{1/2} Re_o^{1/3}$	$Re < 2100$	Leibson *et al*. (1958)	Kantarci *et al* (2005)
$d_b = 0.28 Re_o^{-0.05}$	$Re > 10000$	Leibson *et al*. (1958)	Leibson *et al*. (1958)
$V_b = \left(\frac{4\pi}{3}\right)^{1/3} \left(\frac{15\mu_l Q}{2\rho_l g}\right)$	--------	Kumar and Kuloor (1970)	Kantarci *et al* (2005)
$d_b = 1.817 \left[\frac{\sigma d_o}{g(\rho_l - \rho_g)}\right]^{1/3}$	Valid for low gas flow rate.	Van Krevelen & Hoftijizer, (1950)	Miller (1974)
$d_b = 1.56 Re_o^{0.058} \left(\frac{\sigma d_o^2}{(\rho_l - \rho_g) g}\right)^{0.25}$	$1 < Re < 10$	Kumar *et al*. (1976)	Painmanakul *et al.* (2009)
$d_b = 0.32 Re_o^{0.425} \left(\frac{\sigma d_o^2}{(\rho_l - \rho_g) g}\right)^{0.25}$	$10 < Re < 2100$	Kumar *et al*. (1976)	Painmanakul *et al.* (2009)
$d_b = 100 Re_o^{-0.4} \left(\frac{\sigma d_o^2}{(\rho_l - \rho_g) g}\right)^{0.25}$	$4000 < Re < 70000$	Kumar *et al*. (1976)	Kumar *et al*. (1976)
$\frac{d_b}{d_o} = 3.23 \left(\frac{4\rho_l Q}{\pi \mu_l d_o}\right)^{-0.1} \left(\frac{Q^2}{d_o^5 g}\right)^{0.21}$	--------	Bhavaraju *et al*. (1978)	Kantarci *et al*. (2005)
$d_b = 0.19 d_o^{0.48} Re_o^{0.32}$	$Re < 2000$	Moo-Young and Blanch (1981)	Kantarci et al (2005)
$\frac{g\rho_l d_b^2}{\sigma} = 8.8 \left(\frac{U_g \mu_l}{\sigma}\right)^{-0.04} \left(\frac{\sigma^3 \rho_l}{g\mu_l^4}\right)^{-0.12} \left(\frac{\rho_l}{\rho_g}\right)^{0.22}$		Wilkinson *et al*. (1994)	Painmanakul *et al*. (2009)

Chapter 3: Experimental Design and Methodology

Two experimental setups were used to perform the oxygenation and the bubble hydrodynamics testing for a single orifice with different sizes. The first setup tested the oxygenation performance while the second setup was for determining the bubble size, frequency and rising velocity by means of high speed camera. The non-steady state gas transfer methodology was adopted for calculating volumetric mass transfer coefficient KLa.

3.1. Experimental Setups

3.1.1. Single Orifice Setup

A PVC pipe with 3-inch diameter and 60-inch height was employed to perform the single orifice study. Five different aspect ratios and flow rates, in the range of 6 – 18 and 0.05 – 0.15 SLPM respectively, were investigated. Seven orifice sizes in the range of 0.2 – 0.61 mm were tested under the abovementioned conditions, except for the 0.2 mm orifice where only 6, 9, 12 and 18 aspect ratios have been tested, to be a total 170 experiments. A Vernier DO probe was used to measure the dissolved oxygen concentration in water within the range of 0 to 20 mg/l and 1% accuracy. The obtained readings were collected using a data acquisition system at a frequency of 1 Hz, in addition to its capability to self-calibrate data relying on atmospheric pressure and water temperature obtained by integrated sensors. This allowed oxygen saturation level and saturation percentage determination. Table 3-1 summarizes the studied parameters and the number of tests performed for each orifice size.

Table 3-1: The testing conditions for the aeration efficiency prediction study.

d_o (mm)	Q^* (SLPM)	Aspect Ratio	No. of Experiments
0.2	0.05 – 0.15	6,9,12 and 18	20
0.25	0.05 – 0.15	6, 9, 12, 15 and 18	25
0.3	0.05 – 0.15	6, 9, 12, 15 and 18	25
0.34	0.05 – 0.15	6, 9, 12, 15 and 18	25
0.41	0.05 – 0.15	6, 9, 12, 15 and 18	25
0.51	0.05 – 0.15	6, 9, 12, 15 and 18	25
0.61	0.05 – 0.15	6, 9, 12, 15 and 18	25
		Total	**170**

***A flow rate step of 0.025 SLPM.**

As precise measurement of air characteristics was needed, Omega digital flow meter (Model FMA-2600A) was employed to accurately measure volumetric air flow rate (LPM) with a resolution of 0.2% from the full scale and 0.8% of reading for the latter. The resulting volumetric flow rate (LPM) reading was compensated depending on the operational air pressure and temperature to obtain the standard flow rate value (SLPM). Additionally, the flow meter was equipped with a control valve to precisely adjust air flow rate as required. Figure 3-1 shows a schematic diagram of the single orifice setup components.

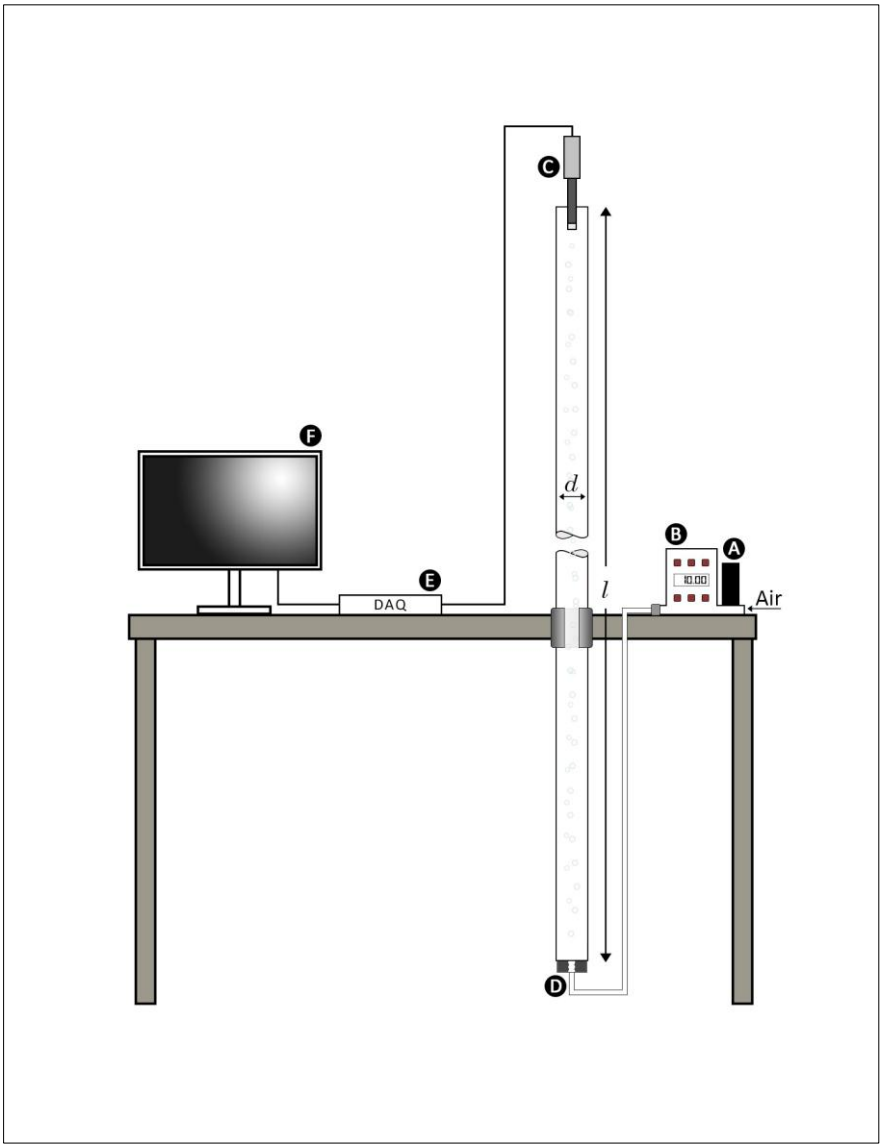

Figure 3-1: Single orifice setup: A: Control Valve, B: Digital Mass Flow Meter, C: DO Probe, D: PVC cap with single orifice, E: Data Acquisition and F: Computer.

3.1.2. Bubble Formation Setup

A glass tank (30”×12”×18”) was used to observe bubble formation under a 16” water height by means of Photron UX 50 Monochrome high speed camera which has a resolution of 1 Mega pixels when recording at a frame rate less or equal to 2000 FPS. The same air flow meter that was described earlier was also used in this apparatus for mass air flow rate measurements.

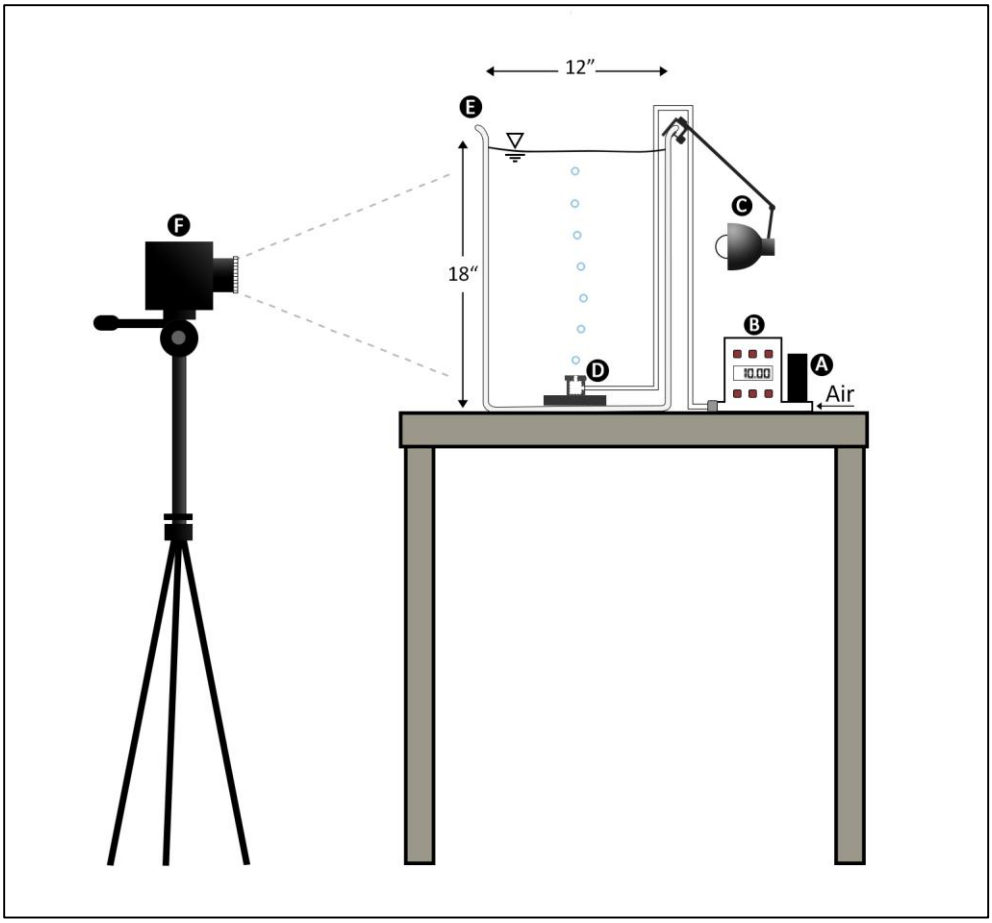

Figure 3-2: Bubble hydrodynamics setup: A: Control Valve, B: Digital Flow Meter, C: Lighting, D: Single Orifice Base, E: Transparent Tank and F: High Speed Camera.

3.2. Experimental Procedure

3.2.1. Non Steady State Aeration

Testing aeration systems has simply two steps: deoxygenate testing water and re-aeration while recording DO concentration. The de-oxygenation process is achieved by adding Sodium Sulfite (Na_2SO_3) to the water with the presence of Cobalt Chloride catalyzer in an adequate concentration, typically 0.1 to 0.5 mg/l. The Sodium Sulfite reacts with the dissolved oxygen in water to produce Sodium Sulfate (Na_2SO_4) according to the following chemical reaction:

$$2Na_2SO_3 + O_2 \xrightarrow{CoCl_2} 2Na_2SO_4$$

Theoretically, 7.88 mg/l of Sodium Sulfite is needed to deoxygenate 1 mg/l of dissolved oxygen concentration. An excess amount of Sodium Sulfite is usually added with the increase of air flow rate and to compensate any partial oxygenation may occur during mixing. This extra amount may be added up to 250% of the stoichiometric amount (ASCE, 1993). However, adding an excessive amount of Na_2SO_3 results in an elevated total dissolved solid (TDS) solutions, which causes an increase in oxygen mass transfer. To avoid irregularities in data caused by Sodium Sulfite accumulation, new fresh water was used for each experiment. In addition, the first run in each new water fill was neglected because of the inconsistency in its outcomes (Huibregtse, Rooney, & Rasmussen, 1983), and was done to allow Cobalt Chloride distribution before actual testing started. After the deoxygenation of water, reaeration started and the dissolved oxygen concentration was monitored by the DO probe and recorded to a computer using a data acquisition system.

3.2.2. Bubble Hydrodynamics

Nedeltchev and Schumpe (2011) have mentioned four methods used for measuring mean bubble diameter, namely: the photographic method (as in Leibson *et al.* (1958) and Wilkinson *et al.* (1994)), the chemical area method (as in Kumar *et al.* (1976)), optical fiber method, and electroresistivity method. In the present study, the photographic technique was utilized to measure the bubble size by virtue of its simple and easy measurement procedure (Wilkinson & Haringa, 1994). The high speed camera was fixed perpendicularly to the glass tank to capture the bubble formation form a single orifice that was placed at its bottom. A ruler was fixed on the same plane of the orifice cap to allow pixel size

calibration for the captured videos, as described in Fayolle, *et al*. (2010). After video capturing, the bubble diameter, frequency and average velocity were analyzed using PFV software as will be illustrated in the following section.

3.3. Data Analysis

3.3.1. Oxygen Transfer and Aeration Efficiency Calculations

The oxygen mass transfer is dependable on the difference of oxygen concentration. The dissolved oxygen concentration (in mg/l) was monitored during the aeration process by DO probe, as described previously. The data obtained were analyzed to find the volumetric mass transfer coefficient KLa, according to the following equation:

$$KLa = ln(\frac{C_\infty - C}{C_\infty - C_0})/t \quad (3\text{-}1)$$

The standard conditions defined for oxygen mass transfer process are: water temperature of 20°C, atmospheric pressure of 14.71 PSIA and an initial oxygen concentration of zero mg/l. However, it is hard to control all these parameters during the aeration test. Therefore, correction factors are applied to the volumetric mass transfer coefficient to get the standard oxygen transfer coefficient KLa_{20}. According to the ASCE (1993), the temperature correction is as follow:

$$KLa_{20} = KLa \times 1.024^{(20-T)} \quad (3\text{-}2)$$

Next, the Oxygen transfer rate can be calculated using the two film theory as follow (with zero initial concentration is assumed):

$$SOTR = KLa_{20} C_\infty V_w \quad (3\text{-}3)$$

In addition, a dimensionless parameter called the standard oxygen transfer efficiency (SOTE) shows the effectiveness of an aeration system in transferring oxygen to water.

SOTE is defined as the ratio of the standard oxygen transfer rate (SOTR) to the mass flow rate of oxygen supplied to the system:

$$SOTE = \frac{SOTR}{\dot{W}_{O_2}} \times 100\% \quad (3\text{-}4)$$

The main interest of this research was to calculate the Standard Aeration Efficiency (SAE) of systems that were studied. The standard aeration efficiency is defined as the ratio of standard oxygen transfer rate (SOTR) to the power consumed (P).

$$SAE = \frac{SOTR}{P} \quad (3\text{-}5)$$

Where the break power (P) can be calculated as follow:

$$P = Qp \quad (3\text{-}6)$$

3.3.2. Bubble Hydrodynamic Properties

Because an elliptic bubble shape was obtained, the major axis a and the minor axis b were measured to evaluate their equivalent diameter d_{eq} according to Eq. (3-7) (Pittoors & Guo, 2014a). Following the equivalent bubble determination, Sauter mean bubble diameter d_b was calculated for each experiment according to Eq. (3-8). The bubble average velocity was also obtained simply by dividing the vertical travel distance over the travel time, as in Eq. (3-9).

$$d_{eq} = \sqrt[3]{a^2 b} \quad (3\text{-}7)$$

$$d_b = \frac{\sum_{i=1}^{N} d_{eq}^3}{\sum_{i=1}^{N} d_{eq}^2} \quad (3\text{-}8)$$

$$U_b = d/t \quad (3\text{-}9)$$

In regards to bubble frequency, it was computed by dividing the number of bubbles (N_b) generated and detached from the orifice over the total time of photographing (t) as

in Eq (3-10). Counted bubbles were attributed to three stages: nucleus formation, bubble detachment, and rise till the evolution of a new bubble; which corresponded to two well-known times: formation time and waiting time. Figure 3-3 shows a schematic diagram that illustrates the hydrodynamics measurements.

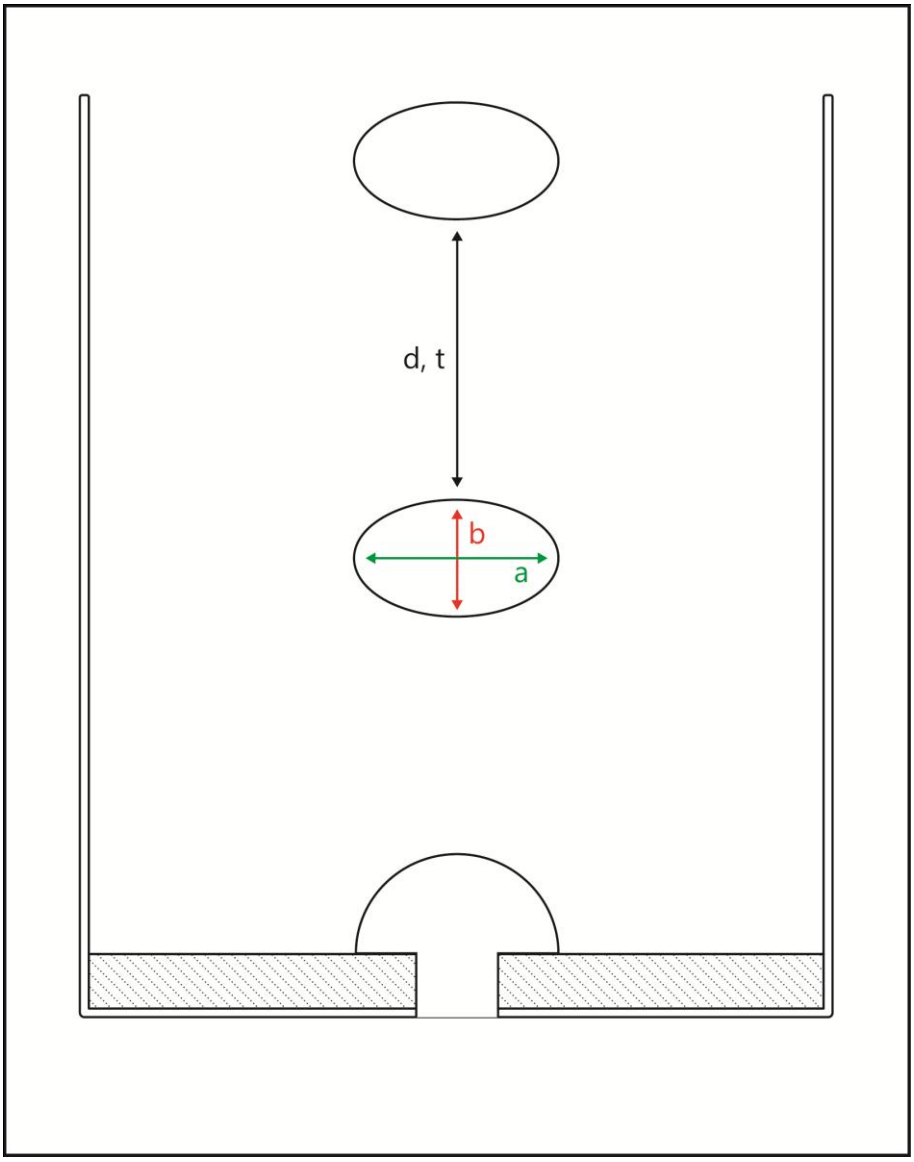

Figure 3-3: Illustrative schematic diagram for hydrodynamics measurements.

Successive frames captured by the camera were used to calculate the total recording time of generated bubbles depending on the specified frame rate ($\dot{F}$), and the starting frame (F_s) and ending frame (F_e).

$$f_b = N_b/t \tag{3-10}$$

$$t = (F_e - F_s)/\dot{F} \tag{3-11}$$

Chapter 4: Air Bubble Size and Frequency Prediction

Hydrodynamics and physicochemical properties are of utmost interest in studying bubble formation in a continuous liquid phase. The highest attention is concentrated on bubble diameter because of its vital role in improving mass transfer and its influence on the other hydrodynamic properties (Painmanakul, Wachirasak, Jamnongwong, & Hebrard, 2009). This is clear as the effectiveness of many chemical and manufactural processes depends on the bubble and droplet size (Dietrich, Mayoufi, Poncin, & Li, 2013). Therefore, it is worthwhile to study the affecting parameters of bubble formation, and model predictable correlations of their diameter and the corresponding formation frequency.

4.1. Studied Parameters from Literature

A substantial body of literature exists in this topic. Leibson *et al*. (1958), Kumar and Kuloor (1970), Miller (1974), Kumar *et al*. (1976), Bhavaraju *et al*. (1978), Moo-Young and Blanch (1981), and Wilkinson *et al*. (1994) developed correlations for predicting bubble size for single and multiple orifices, with a various combination of gas and liquid phases. Summarizing the previous work, the orifice Reynolds number is substantial in the bubble formation process. Starting with very low Reynolds numbers, bubble size is mostly governed by the orifice diameter and the Reynolds number has a minimal effect. This first region may be represented by Van Krevelen and Hoftijzer's equation (1950) and Kumar *et al.* (1976) equation for $Re < 10$. With Reynolds number ranging from 10 up to its critical value of 2100, the inertia forces govern bubble formation in addition to the orifice

geometry, and the mean bubble diameter increases with the increase in Reynold number. Finally, bubble formation is only a function of Reynolds number and orifice geometry does not have any considerable effect as described in Leibson *et al.* (1958) and concluded from Miller's (1974) study. The equation developed by Kumar *et al.* (1976) showed significance for orifice diameter even at very high Reynolds numbers.

4.2. Experimental Results

Eleven different orifices with a diameter ranging from 0.2 – 1mm were tested under a standard volumetric flow rate of 0.05 – 0.15 SLPM. The resulted air bubble size and frequency were traced using Photronl UX 50 Monochrome high speed camera. As was expected, the air bubble average diameter increased with higher flow rates and larger orifice size. The bubble frequency, on the other hand, decreased with larger orifice size, but had a proportional increase with elevated flow rates.

As summarized below in Table 4-1, eleven orifices were tested for bubble size and bubble frequency. Each of these orifices were created by drilling through a ½-inch finished surface PVC cap. For orifice sizes ranging from 0.3 to 1.0 mm, the generated bubbles were observed with a flow rate range of 0.05 – 0.15 SLPM, with 0.05 SLPM step, while the 0.2mm and 0.25mm orifice sizes were tested at a flow rate range of 0.05 – 0.1 SLPM and 0.05 – 0.125 SLPM respectively, to be a total of 52 experiments. The corresponding orifice Reynolds number, orifice Weber number, and static to chamber pressure ratio were 69 – 686, 15 – 7716 and 0.34 – 0.98 N/m^2 respectively.

Table 4-1: Testing conditions and results summary.

d_o (mm)	Q^* (SLPM)	d_b (mm)	Re_o	We_o	$\frac{p_s}{p_c}$	No. of Experiments
0.2	0.05 – 0.1	3.7 – 4.4	343 – 686	1929 – 7716	0.58 – 0.34	3
0.25	0.05 – 0.125	3.8 – 4.6	275 – 686	987 – 6173	0.72 – 0.45	4
0.3	0.05 – 0.15	3.9 – 5.0	229 – 686	571 – 5144	0.78 – 0.49	5
0.34	0.05 – 0.15	3.9 – 5.4	202 – 606	392 – 3533	0.80 – 0.69	5
0.41	0.05 – 0.15	4.0 – 5.4	167 – 502	223 – 2015	0.82 – 0.75	5
0.51	0.05 – 0.15	4.7 – 5.9	135 – 404	116 – 1047	0.84 – 0.82	5
0.61	0.05 – 0.15	5.1 – 5.6	113 – 338	68 – 612	0.93 – 0.90	5
0.71	0.05 – 0.15	5.6 – 6.2	97 – 290	43 – 388	0.95 – 0.93	5
0.81	0.05 – 0.15	5.6 – 6.3	85 – 254	29 – 261	0.95**	5
0.91	0.05 – 0.15	5.9 – 6.6	75 – 226	20 – 184	0.96**	5
1.0	0.05 – 0.15	6.2 – 6.9	69 – 206	15 – 139	0.98**	5
					Total	**52**

***A flow rate step of 0.025 SLPM.**
****No significant change in chamber pressure has been detected.**

4.3. Bubble Size Correlation

An empirical formula was established using nonlinear regression as in (Brown, 2001) with a correlation factor of $R^2 = 0.95$ with an average relative error of 2.7%. The formula was capable of predicting the bubble size within $\pm 10\%$ (see Figure 4-1). Equation (4-1) was designed by parameters related to the orifice, making them easier to be measured and calculated.

$$d_b = 0.18\, Re_o^{1.15}\, We_o^{-0.51} \left(\frac{P_s}{P_t}\right)^{-0.213} \tag{4-1}$$

As shown in equation (4-1), orifice Reynolds number was directly proportional to the bubble size with a power of 1.15, while Weber number suppressed the diameter with a power exponent of -0.51. The effect of Reynolds number was unexpected since its high values were associated with smaller bubble size in the tested range, meaning more bubbles if the constant mass flow rate condition was applied. An explanation would be that inertia forces were present in both Reynolds and Weber numbers; the first tends to

enlarge the bubble to accommodate the added air mass, whilst inertia over surface tension force leads to tearing the bubble surface at a faster rate. Final diameter behavior was determined depending on which of them was dominant. The two opposing actions of Re_o and We_o were mostly seen at high flow rates (especially at 0.15 SLPM) when many small bubbles were coexisting with large ones.

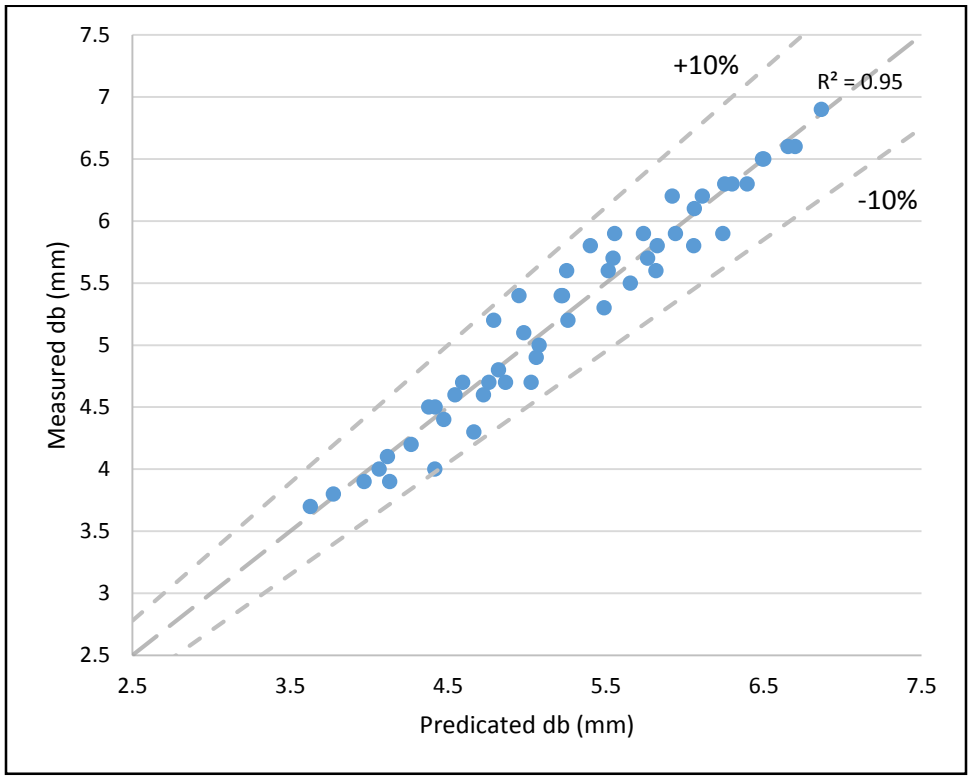

Figure 4-1: Measured and Predicted Values Comparison for Bubble Size.

The pressure ratio between upstream and downstream showed significant contribution to the size of the bubble. Increasing static-to-chamber pressure ratio was found to increase the bubble diameter because the increase in air chamber pressure caused higher output velocity resulting in higher Reynolds number.

4.4. Bubble Frequency Correlation

In an analogous way, bubble frequency equation was developed with a correlation factor of $R^2 = 0.92$ with an average error of 11% (See Figure 4-2). This formula predicts frequency of bubbles within $\pm 25\%$.

$$f_b = 13.2\, Re_o^{-0.4}\, We_o^{0.5} \left(\frac{P_s}{P_t}\right)^{0.65} \tag{4-2}$$

This frequency equation had an opposite trend of the bubble size equation. The increase in Reynolds number had a negative influence on bubble frequency with a power relation of -0.4.

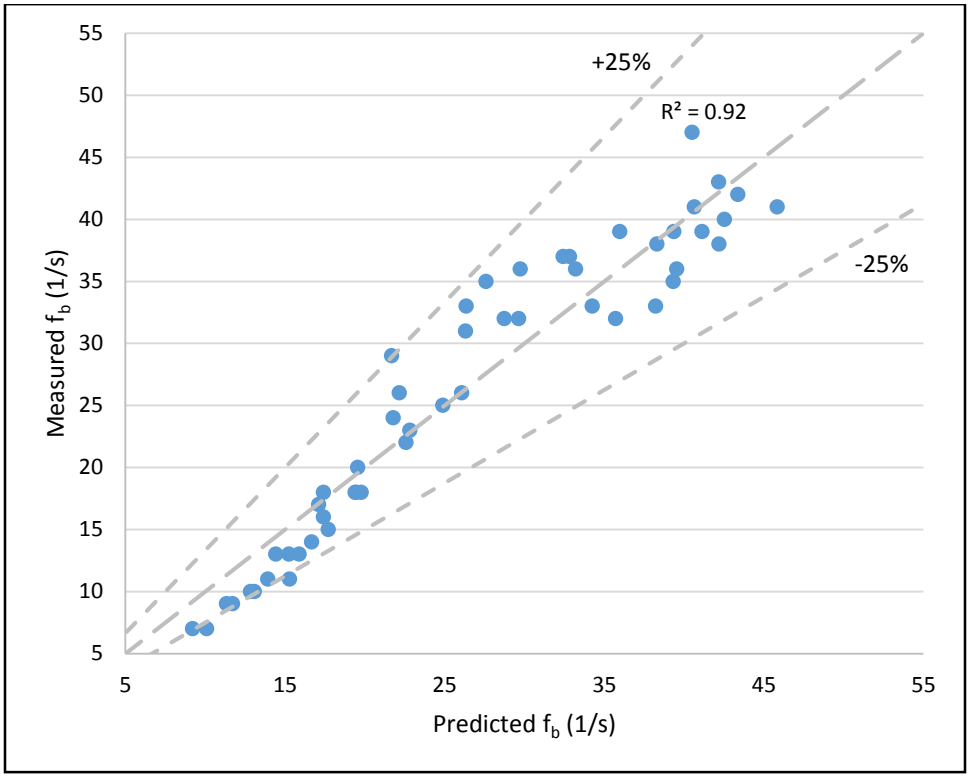

Figure 4-2: Measured and Predicted Values Comparison for Bubble Frequency.

In contrast, the Weber number and static-to-chamber pressure ratio increased the bubble frequency with a power of 0.5 and 0.65 respectively. This positive influence was attributed to the increase in bubble splitting seen with higher Weber numbers in addition

to the higher air velocity at the orifice due to elevated chamber pressure. Moreover, at the same flow rate, smaller orifice diameters generated smaller bubble sizes and, as a result, greater bubble frequency occurred to meet the required flow rate.

Chapter 5: Aeration Efficiency Prediction Formula

Power consumption is a huge concern in WWTPs globally. What mainly makes energy depletion worse is the secondary biological treatment that involves the aeration process. Most literature focus on determining the vital parameters influencing oxygen transfer itself in addition to developing correlations that describe a system's performance, rather than taking energy intake into consideration. This is understandable as improving oxygen mass transfer enhances aeration efficiency and has a directly proportional relation if a constant power withdrawal is assumed. However, most mass transfer enhancement techniques deplete more energy, and as a result, suppress the system's aeration efficiency; especially if the increase in mass transfer coefficient is not comparable to the power consumed. Examples of these techniques are: smaller orifice diameter, additional impeller for agitating aeration tank, bubble shearing mechanism, jet aerators to generate micro bubbles … etc.

Consequently, it is worth investigating the design parameters by establishing a predictable correlation of AE to find the optimum operational conditions.

5.1. Experimental Results

Orifice sizes in the range of 0.2 – 0.61 mm were tested for oxygen transfer under an air flow rate of 0.05 – 0.15 SLPM and submergence height of 18" – 54". Results showed that the peak value of AE was 8.11 KgO_2/KWh at a flow rate of 0.05 SLPM, and 1.37m height for an orifice diameter of 0.3mm. The overall behavior of AE with changing the orifice diameter is illustrated in Figure 5-1.

It is obvious that between 0.3 – 0.41 mm, AE slightly decreased and almost had a plateau shape, but with orifices larger than 0.41mm, a noticeable decline appeared.

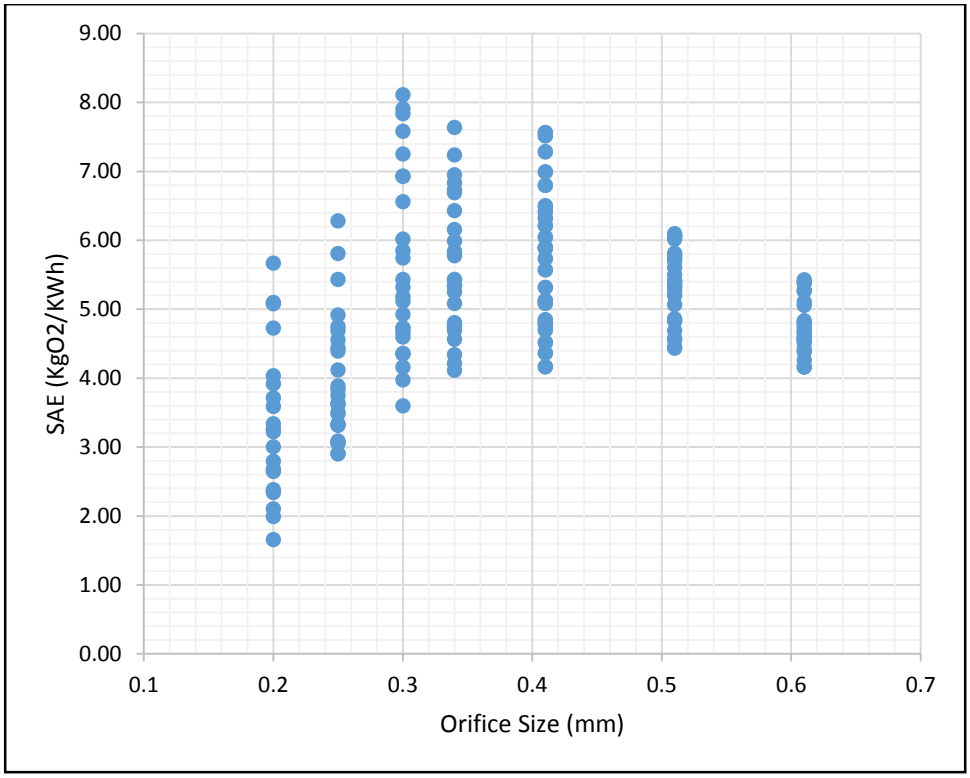

Figure 5-1: the general trend of aeration efficiency with orifice diameter.

5.2. Dimensionless Mathematical Model

The dimensionless analysis is a well-known technique to formulate mathematical models from experimental data, especially if scale-up was desired. Recently, Pittoors *et al*. (2014b), Al-Ahmady (2011), Schierholz *et al*. (2006) and Gillot *et al*. (2005) developed empirical correlations derived from either a real site measurements or lab scale investigations. Summarizing the previous work, 12 parameters control mass transfer in gas-liquid systems, namely: bubble mean diameter, air volumetric flow rate, submergence height, tank dimensions (Height and Diameter), aerated area, diffuser density, tank Reynolds number, tank Froude number, gas superficial velocity, water

viscosity, molecular diffusivity, and air to water ratio. Depending on these parameters, a primary mathematical model for aeration efficiency was developed. Since aeration efficiency includes power consumption, both air chamber pressure and orifice Euler number were also considered in the model as energy consumption is inherently included in them. Table 5-1 shows the parameters and the dimensions for each of them.

$$SAE = f(A_a, A_t, D, D_o, D_b, D_t, g, h_d, h_t, p_c, p_s, Q, U_b, V_w, \rho_g, \nu_w)$$

$$\frac{D^2 SAE}{D_t^2} =$$

$$\emptyset \left(\frac{Q}{D_t \nu_w}\right)^{\emptyset 1} \left(\frac{Q}{\sqrt{D_t^5 g}}\right)^{\emptyset 2} \left(\frac{p_c}{\rho_g}\left(\frac{D_o^2}{\mathrm{Q}}\right)^2\right)^{\emptyset 3} \left(\frac{Q h_d}{V_w U_b}\right)^{\emptyset 4} \left(\frac{h_d}{h_t}\right)^{\emptyset 5} \left(\frac{h_d}{D_t}\right)^{\emptyset 6} \left(\frac{A_a}{A_t}\right)^{\emptyset 7} \left(\frac{p_s}{p_c}\right)^{\emptyset 8} \left(\frac{D_o}{D_b}\right)^{\emptyset 9} \quad (5\text{-}1)$$

$$SAE = \emptyset \left(\frac{D_t}{D}\right)^2 Re^{\emptyset 1} Fr^{\emptyset 2} Eu^{\emptyset 3} \varepsilon_b^{\emptyset 4} \left(\frac{h_d}{h_t}\right)^{\emptyset 5} \left(\frac{h_t}{D_t}\right)^{\emptyset 6} \left(\frac{A_a}{A_t}\right)^{\emptyset 7} \left(\frac{p_s}{p_c}\right)^{\emptyset 8} \left(\frac{D_o}{D_b}\right)^{\emptyset 9} \quad (5\text{-}2)$$

$$SAE = \emptyset \, Re^{\emptyset 1} Fr^{\emptyset 2} Eu^{\emptyset 3} \varepsilon_b^{\emptyset 4} \left(\frac{h_d}{h_t}\right)^{\emptyset 5} \left(\frac{h_t}{D_t}\right)^{\emptyset 6} \left(\frac{A_a}{A_t}\right)^{\emptyset 7} \left(\frac{p_s}{p_c}\right)^{\emptyset 9} \left(\frac{D_o}{D_b}\right)^{\emptyset 9} \quad (5\text{-}3)$$

Table 5-1: A summary of the correlating parameters, their units and dimensions.

Parameter	Symbol	Unit	Dimensional Unit
Aeration Efficiency	SAE	$\frac{KgO_2}{KW.h}$	$\frac{T^2}{L^2}$
Volumetric Mass Transfer Coefficient	KLa_{20}	$\frac{1}{h}$	$\frac{1}{T}$
Water Volume	V_w	m^3	L^3
Air Chamber Pressure	p_c	$\frac{Kg_{Air}}{m.s^2}$	$\frac{M}{T^2L}$
Water Static Pressure	p_s	$\frac{Kg_{Air}}{m.s^2}$	$\frac{M}{T^2L}$
Air Volumetric Flow Rate	Q	$\frac{m^3}{s}$	$\frac{L^3}{T}$
Average Air Bubble Velocity	U_b	$\frac{m}{s}$	$\frac{L}{T}$
Air Density	ρ_g	$\frac{Kg_{Air}}{m^3}$	$\frac{M}{L^3}$
Oxygen Mass Flow Rate	$\dot{W}_{O_2}$	$\frac{Kg_{O_2}}{s}$	$\frac{M}{T}$
Oxygen Diffusion Coefficient	D	$\frac{m^2}{s}$	$\frac{L^2}{T}$
Orifice Diameter	d_o	m	L
Bubble Avg. Diameter	d_b	m	L
Submergence Height	h_d	m	L
Tank Diameter	D_t	m	L
Tank Height	h_t	m	L
Aerated Area	A_a	m^2	L^2
Tank Area	A_t	m^2	L^2
Water Kinetic Viscosity	ν_w	$\frac{m^2}{s}$	$\frac{L^2}{T}$
Tank Reynolds Number	$Re = \frac{Q}{D_t \nu_w}$	-	-
Tank Froude Number	$Fr = \frac{Q}{\sqrt{D_t^5 g}}$	-	-
Orifice Euler Number	$Eu = \frac{p_c}{\rho_g}\left(\frac{d_o^2}{Q}\right)^2$	-	-
Gas Hold-up	$\varepsilon_b = \frac{Q h_d}{V_w U_b}$	-	-

5.3. Aeration Efficiency Predicting Formula

As in chapter four, nonlinear regression was utilized to establish a correlation for predicting the aeration performance by numerically calculating exponents of the parameters using SOLVER function as in (Brown, 2001). The best correlation developed had a correlation factor of $R^2 = 0.94$ for the data between 0.2 – 0.41 mm with an average relative error of 5.4% (predicts within $\pm 20\%$). When all the studied region was considered for modeling, the correlation factor decreased, making the formula unpredictable. The ranges of studied parameters are summarized in Table 5-2 below.

Table 5-2: Range of studied variables of orifice size range of (0.2 – 0.41mm).

Parameter	Range Studied
Flow Rate	0.05 – 0.15 (SLPM)
Orifice Diameter	0.2 – 0.41 (mm)
Bubble Size	3.70 – 5.40 (mm)
Water Volume	2.20 – 6.60 (L)
Gas Holdup	4.51E-04 – 1.40E-03
Static to Chamber Pressure Ratio	0.19 – 0.94
Aerated Area to Tank Area Ratio	0.30 – 0.58
Tank Aspect Ratio	6 - 18
Diffuser Submergence Height	0.46 – 1.37 (m)
Orifice to bubble size ration	0.04 – 0.10
Aeration Efficiency	1.66 – 8.11 ($\frac{KgO_2}{KW.h}$)
Volumetric Mass Transfer Coefficient	1.31– 5.57 ($\frac{1}{h}$)

The twelve influencing parameters were investigated in this study. However, only 5 of them were found to have the most significance in predicting AE. These parameters are: gas holdup, static-to-chamber pressure ratio, tank aspect ratio, orifice diameter to bubble diameter ratio and aerated area to tank area ratio.

Equation (5-4) is the final model after neglecting all insignificant parameters, as will be elaborated in the following sections. The predicted and measured values of aeration efficiency are presented in Figure 5-2.

$$SAE = 0.541\ \varepsilon_b^{-0.449} \left(\frac{p_s}{p_c}\right)^{0.721} \left(\frac{h_d}{D_t}\right)^{-0.082} \left(\frac{d_o}{d_b}\right)^{0.123} \left(\frac{A_a}{A_t}\right)^{0.201} \quad (5\text{-}4)$$

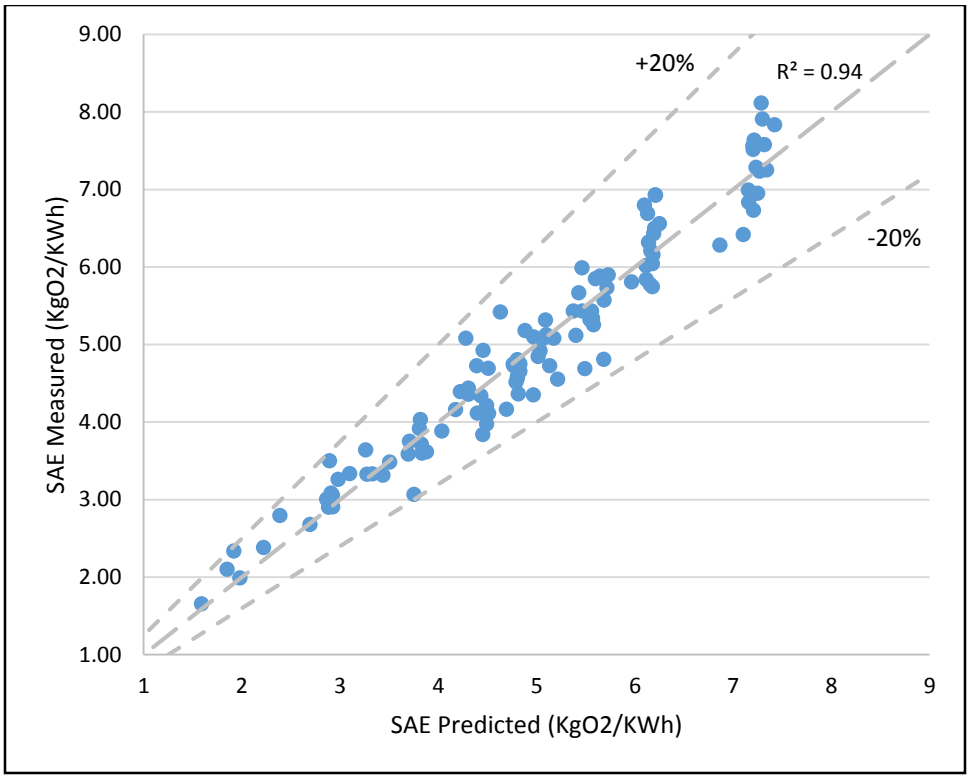

Figure 5-2: Aeration Efficiency Comparison between Measured and Predicted Values.

5.4. Discussion

5.4.1. Gas-Holdup

Gas holdup is defined as the ratio of the amount of air that coexists with water at a certain instant. It is the best parameter that reflects the ratio between air and water in a bubbly flow system, in addition to its influence on mass transfer (Li, Zeng, & Fan, 2008).

$$\varepsilon_b = \frac{Q h_d}{V_w U_b} \quad (5\text{-}5)$$

The submergence height and bubble velocity are also included in the gas hold up equation. These two factors are crucial on the mass transfer process, as bubble travel time inside the column is dependent on them (Ashley, Mavinic, & Hall, 2009). Since the diameter of tank was constant in this study, Eq. (5-5) can be further simplified to be as follows:

$$\varepsilon_b = \frac{Q}{\pi D_t^2 U_b} \tag{5-6}$$

Measuring the bubble velocity showed small variations in its value and ranged from 0.31 – 0.39 m/s, making the gas hold up nearly a function of volumetric flow rate. Increasing volumetric flow rate is known to be a critical factor in enhancing mass transfer coefficient. However, it is worth noting that higher volumetric flow rate also means greater energy depletion. As a result, gas holdup impact on AE was represented as a negative exponent of 0.449 in the developed equation. This decrease in AE is explained as the enhancement from increasing mass transfer is much less than the power needed to operate an aeration system at such conditions.

5.4.2. Static to Chamber Pressure Ratio

Both Euler number and static to chamber pressure ratio were considered as indicators of the extent of power consumption. After investigating both parameters, however, better prediction was obtained in the case of pressure ratio; therefore, it was considered in the final model instead of Euler number. In addition, it is easier to measure both air chamber pressure and static pressure than calculate Euler number. Furthermore, Euler number requires more calculations of orifice air velocity as discharge coefficient might be included, making the calculation difficult and probably inaccurate.

Referring to the experimental results, a significant influence of air chamber pressure was noticed at relatively small orifice size, as was expected. This decrease is attributed to the elevated chamber pressure at such small orifices. In addition, the developed correlation from experimental results showed that the pressure ratio had the largest impact on AE with a power exponent of 0.721.

5.4.3. Submergence Height to Tank Diameter Ratio

A slight contribution was noticed for tank aspect ratio with a negative power relationship. This negative behavior is attributed to the submergence height as higher water level means higher static pressure. Considering previous correlations, like Gillot *et al.* (2005) and Pittoors *et al.* (2014a), water height to tank diameter ratio showed larger effect on oxygen mass transfer because of the various geometrical parameters that were investigated in their studies; unlike the present study where tank diameter was constant. Moreover, the previous studies investigated the effect of the mass transfer coefficient, which is different from studying AE.

5.4.4. Orifice to Bubble Size Ratio

The most important parameter in the mass transfer process is the interfacial area between gas and liquid phases, which depends mainly on bubble diameter. The ratio of the bubble to orifice diameter showed a moderate effect on predicting AE. However, the largest effect of orifice size is inherent in the static to chamber pressure ratio as higher air chamber pressure is associated with smaller orifice size, if the same mass flow rate

was applied. In addition, orifice size governs the bubble formation that is a critical factor in mass transfer.

5.4.5. Aerated to Tank Area Ratio

The aerated area is defined as the area of the air column inside the water. Greater aerated area is an important factor in enhancing mass transfer because more air distribution inside water enhances interfacial area. Moreover, a better prediction was obtained for aeration performance with the existence of this parameter. Likewise, higher diffuser density was proven to have higher transfer efficiency (Gillot, Capela-Marsal, Roustan, & Heduit, 2005). For these reasons, the aerated area was taken into consideration in this study and was normalized to the tank area. The aerated to tank area ratio showed positive impact on the AE with an exponent relation of 0.203. This parameter was also studied by Pittoors *et al.* (2014a), Al-Ahmady (Al-Ahmady, 2011) and Gillot *et al.* (2005) and showed a significant contribution in oxygenation process.

5.4.6. Other Studied Parameters

Tank Reynolds number and tank Froude number have not shown any significance as Pittoors *et al.* (2014b) and Al-Ahmady (2011) have noted. Dissimilar to their studies, dimensions of the testing tank were not changed in the present study and, therefore, no noticeable effect was found. However, tank Reynolds number and tank Froude number are crucial in representing tank mixing and should be studied extensively in further investigations.

Chapter 6: Conclusions

The main purpose of this study was to establish an empirical model for aeration efficiency from a lab-scale experiments through testing single orifices with various diameter sizes. In addition, it was necessary to study the bubble hydrodynamics for the tested orifice, because of their importance in calculating essential parameters for AE. The following two sections provide the main conclusions that were drawn from these studies.

6.1. Hydrodynamics Study

Eleven different single orifices in the range of 0.2 – 1.0 mm were tested for bubble size and frequency by means of high speed camera to formulate two new predictable correlations:

$$d_b = 0.18\, Re_o^{1.15}\, We_o^{-0.51} \left(\frac{p_s}{p_c}\right)^{-0.213}$$

$$f_b = 13.2\, Re_o^{-0.4}\, We_o^{0.5} \left(\frac{P_s}{P_t}\right)^{0.65}$$

Flow rate and orifice size have the highest impact on the bubble size and frequency, which are represented by the Weber and Reynolds Numbers. Elevating flow rate proportionally increased the Sauter mean diameter in the range studied as well as the bubble frequency for a constant orifice diameter. Maintaining constant flow rate at smaller perforate size generated smaller bubble size but higher bubble frequency to accommodate the applied volumetric flow rate. In addition, the higher velocity with smaller orifice increased the orifice Weber number that reduced the bubble size and, as a result, enhanced the bubble frequency.

Moreover, static-to-chamber pressure ratio showed a significant contribution in predicating bubble mean diameter and frequency with a power relation of -0.214 and 0.65, respectively.

6.2. Aeration Efficiency Prediction

Single orifices with a diameter ranging from 0.2 – 0.61mm were tested under various submergence heights and standard volumetric flow rates. Results showed that the highest aeration efficiency was achieved at orifice diameter of 0.3 under a flow rate of 0.050 SLPM and 1.37m height. This conclusion was drawn after accomplishing 170 different experiments.

Moreover, an empirical formula was established using the data collected from 0.2 – 0.41mm orifice size by means of nonlinear regression as described in (Brown, 2001). Five parameters from the twelve parameters discussed represented significant contribution during establishing the empirical formula. These factors are: The gas holdup, static to chamber pressure ratio, submergence height to tank diameter ratio, aerated to tank area ratio and orifice to bubble diameter ratio.

$$SAE = 0.541\ \varepsilon_b^{-0.449} \left(\frac{p_s}{p_c}\right)^{0.721} \left(\frac{h_d}{D_t}\right)^{-0.082} \left(\frac{d_o}{d_b}\right)^{0.123} \left(\frac{A_a}{A_t}\right)^{0.201}$$

Both gas hold up and tank aspect ratio influenced negatively the aeration efficiency, while remaining parameters have positive power exponents, with the static-to-chamber pressure ratio having the largest exponent. It is worth noting that the influence of the static-to-chamber pressure ratio on AE has not been studied in literature previously.

Raised volumetric flow rate decreases AE due to higher energy withdrawal. A similar trend is also noticed with higher gas holdup as it is almost a function of flow rate since the tank diameter was constant and bubble velocity did not vary noticeably. Greater static pressure has also a negative impact on energy consumption because higher differential pressure by air blower is needed.

Aerated area gained a significant attention in previous literature. The present study has considered this factor in the developed model by virtue of its oxygen transfer enhancement. As expected, higher aerated area increased aeration efficiency a power relation of 0.201.

Finally, bubble diameter and orifice size are of utmost interest in studying bubble formation and mass transfer coefficient in gas-liquid system. The effect of orifice size is substantial in this study. Bubble size and air chamber pressure are mainly affected by changing orifice diameter. These two variables, bubble size and air chamber pressure, are the most weighted parameters influencing the mass transfer coefficient (represented by bubble size), and the power consumption (represented by the air chamber pressure). Both mass transfer coefficient and power consumption are the principal factors of aeration efficiency, which explains the importance of the orifice diameter in determining the efficiency of an air diffused system.

References

Al-Ahmady, K. (2011). Mathematical Model for Calculating Oxygen Mass Transfer Coefficienct in Diffused Air Systems. *Al-Rafidain Engineering, 19*(4), 43-54.

ASCE. (1993). *Mearuement of Oxygen Transfer in Clean Water.* ASCE.

Ashley, K., Mavinic, D., & Hall, K. (1990). Effects of Orifice Size and Surface Conditions on Oxygen Transfer in A Bench Scale Diffused Aeration System. *Environmental Technology, 11*, 609-618.

Ashley, K., Mavinic, D., & Hall, K. (2009). Effect of Orifice Diameter, Depth of Air Injection and Air Flow Rate on Oxygen Transfer in a Pilot-Scale, Full Lift, Hypolimnetic Aerator. *Canadian Journal of Civil Engineering, 36*, 137-147.

Bhavaraju, S. M., Mashelkar, R. A., & Blanch, H. W. (1978). Bubble motion and mass transfer in non-Newtonian fluids: Part I. Single bubble in power law and Bingham fluids. *AlChE Journal, 24*(6), 1063-1070.

Brown, A. (2001). A Step-by-step Guide to Nonlinear Regressiom Analysis of Experimental Data Using a Microsoft Excel Spreadsheet. *Computer Methods and Programs in Biomedicine, 65*, 191-200.

Capela, S. (1999). *Influence of design factors and operating conditions of activated sludge processes on oxygen transfer.* Paris, France: The`se de Doctorat, Universite´ Paris XII,.

Davis, M. L. (2010). *Water and Wastewater Engineering.* McGraw-Hill.

DeMower, C., Schierholz, E., Gulliver, J., & Wilhelms, S. (2003). Impact of Bubble and Free Surface Oxygen Transfer on Diffused Aeration Systems. *Water Research, 37*(8), 1890-1904.

Dietrich, N., Mayoufi, N., Poncin, S., & Li, H.-Z. (2013). Experimental Investigation of Bubble and Drop Formation at Submerged Orifices. *Chemical Papers, 67*(3), 313-325.

EPA. (1999). *Wastewater Technology Fact Sheet: Fine Bubble Aeration.* Washington, DC: Enviromental Agency Protection.

EPA. (2000). *Decentalized Systems Technology Fact Sheet: Aerobic Treatment.* Washington, DC: EPA.

EPA. (2004). *Wastewater Technology Fact Sheet: Screening and Grit Removal.* Washington, DC: Municipal Technology Branch, U.S. EPA.

Fayolle, Y., Gillot, S., Cockx, A., Bensimhon, L., Roustanb, M., & Heduit, A. (2010). In Situ Characterization of Local Hydrodynamic Parameters in Closed Loop Aeration Tanks. *Chemical Engineering Journal, 158*(2), 207-212.

Gillot, S., Capela-Marsal, S., Roustan, M., & Heduit, A. (2005). Predicting oxygen transfer of fine bubble diffused aeration systems---model issued from dimensional analysis. *Water Research, 39*, 1379-1387.

Gnyloskurenko, S., Byakova, A., Raychenko, O., & Nakamura, T. (2003). Influence of wetting conditions on bubbles formation at orifice in an inviscid liquid.

Transformation of bubble shape and size. *Colloids and Surfaces A: Physicochemical and Engineering Aspects, 218*(1), 73-87.

Huibregtse, G. L., Rooney, T. C., & Rasmussen, D. C. (1983). Factors Affecting Fine Bubble Diffused Aeration. *Water Pollution Control Federation, 55*(8), 1057-1064.

Kantarci, N., Borak, F., & Ulgen, K. (2005). Review: Bubble Coulmn Reactor. *Process Biochemistry, 40*, 2263-2283.

Kumar, A., Degaleesan, T., Laddha, G., & Hoelscher, H. (1976). Bubble Swarm Characteristics in Bubble Columns. *The Canadian Journal of Engineering, 54*(5), 503-508.

Kumar, R., & Kuloor, N. (January de 1970). The Formation of Bubbles and Drops. *Advances in Chemical Engineering, 8*, 256-368.

Leibson, I., Holcomb, E. G., Cacoso, A. G., & Jacmic, J. J. (September de 1958). Rate of Rlow and Mechanics of Bubble Formation from Single Submerged Orifices. II. Mechanics of bubble formation. *AIChE Journal, 2*(3), 296-300.

Lewis, W., & Whitman, W. (1924). Principles of Gas Transfer Absorption. *Industrial and Engineering Chemistry, 16*(12), 1215-1220.

Li, E., Zeng, X., & Fan, Y. (2008). Air-Water Ratio as a Characteristic Criterion for Finr Bubble Diffused Aeration Systems. *Chemical Engineering Journal, 137*, 214-224.

Mavinic, D., & Bewtra, J. (1976). Efficiency of Diffused Aeration Systems in Wastwater Treatment. *Water Pollution Control Federation, 48*(10), 2273-2283.

Metcalf and Eddy, Inc. (1979). *Wastewater Engineering: Treatment, Disposal and Reuse.* McGraw-Hill.

Miller, D. (1974). Scale-up of Agitated Vessels Gas–Liquid Mass transfer. *AIChE Journal, 20*, 445-453.

Moo-Young, M., & Blanch, H. (1981). Design of Biochemical Reactors Mass Transfer Criteria for Simple and Complex Systems. *Advances in Biochemical Engineering, 19*, 1-69.

Nedeltchev, S., & Schumpe, A. (2011). New Approaches for Theoretical Estimation of Mass Transfer Parameters in Both Gas-Liquid and Slurry Bubble Columns. En E. Mohamed (Ed.), *Mass Transfer in Multiphase Systems and its Applications.* In Tech.

Painmanakul, P., Wachirasak, J., Jamnongwong, M., & Hebrard, G. (2009). Theoretical Prediction of Volumetric Mass Transfer Coefficient (KLa) for Designing an Aeration Tank. *Engineering Journal, 13*(3), 13-28.

Pittoors, E., & Guo, Y. V. (2014a). Oxygen Transfer Model Development Based on Activated Sludge and Clean Water in Diffused Aerated Cylinderical Tank. *Chemical Engineering Journal, 243*, 51-59.

Pittoors, E., Guo, Y., & Van Hulle, S. W. (2014b). Modeling Dissolved Oxygen Concentration for Optimizing Aeration Systems and Reducing Oxygen Consumption in Activated Sludge: A Review. *Chemical Engineering Communications*, 983-1002.

Schierholz, E., Gulliver, J., Wilhelms, S., & Henneman, H. (2006). Gas Transfer from Air Diffuser. *Water Research, 40*, 1018-1026.

Solomon, C., Casey, P., Mackne, C., & Lake, A. (1998). *Fine bubble Aeration: A General Overview.* The National Small Flows Cleaninghouse.

Stenstorm, M., & Vazirinejad, H. (1984). Economic Evaluation of Upgrading Aeration Systems. *Water Pollution Control Federation, 56*(1), 20-26.

Van Krevelen, D., & Hoftijizer, P. (1950). Studies of Gas-Bubble Formation: Calculations of Interfacial Area in Bubble Contactors. *Chemical Engineering Progress, 46*(1), 29-35.

Wilkinson, P. M., & Haringa, H. (1994). Mass Transfer and Bubble Size in Bubble Column Under Pressure. *Chemical Engineering Science, 49*(9), 1417-1427.

Appendices

Appendix A: Bubble Hydrodynamics Calculations

Orifice Size (mm)	*Flow Rate (SLPM)*	*Chamber Pressure (PSI)*	D_b *(mm)*	f_b *(s^{-1})*	Re_o	We_o	p_s/p_c	D_b *Predicted (mm)*	f_b *Predicted (s-1)*
0.2	0.05	0.91	3.7	33	343	1929.15	0.58	3.6	39
0.2	0.075	1.2	4	41	515	4340.60	0.44	4.1	42
0.2	0.1	1.57	4.4	47	686	7716.62	0.34	4.5	42
0.25	0.05	0.74	3.8	33	275	987.73	0.72	3.8	35
0.25	0.075	0.86	4.1	36	412	2222.39	0.62	4.1	41
0.25	0.1	1	4.5	40	549	3950.91	0.53	4.4	44
0.25	0.125	1.19	4.6	42	686	6173.30	0.45	4.7	45
0.3	0.05	0.68	3.9	32	229	571.60	0.78	4.0	31
0.3	0.075	0.74	4.2	32	343	1286.10	0.72	4.3	37
0.3	0.1	0.83	4.6	35	458	2286.41	0.64	4.5	41
0.3	0.125	0.95	4.8	39	572	3572.51	0.56	4.8	43
0.3	0.15	1.08	5	43	686	5144.41	0.49	5.1	44
0.34	0.05	0.66	3.9	33	202	392.66	0.80	4.1	27
0.34	0.075	0.67	4.5	36	303	883.49	0.79	4.4	34
0.34	0.1	0.7	4.7	38	404	1570.65	0.76	4.6	40
0.34	0.125	0.74	5.2	38	505	2454.15	0.72	4.8	44
0.34	0.15	0.77	5.4	41	606	3533.97	0.69	4.9	47
0.41	0.05	0.65	4	29	167	223.93	0.82	4.4	22
0.41	0.075	0.65	4.3	35	251	503.83	0.82	4.7	28
0.41	0.1	0.66	4.7	37	335	895.71	0.80	4.9	33
0.41	0.125	0.69	4.9	39	419	1399.54	0.77	5.1	37
0.41	0.15	0.71	5.4	39	502	2015.34	0.75	5.2	41
0.51	0.05	0.63	4.7	18	135	116.34	0.84	4.8	18
0.51	0.075	0.63	4.7	26	202	261.78	0.84	5.0	23
0.51	0.1	0.63	5.4	31	269	465.38	0.84	5.2	27
0.51	0.125	0.64	5.8	36	337	727.15	0.83	5.4	31
0.51	0.15	0.65	5.9	37	404	1047.10	0.82	5.6	34
0.61	0.05	0.57	5.1	11	113	67.99	0.93	5.0	16

Orifice Size (mm)	*Flow Rate (SLPM)*	*Chamber Pressure (PSI)*	D_b *(mm)*	f_b *(s^{-1})*	Re_o	We_o	p_s/p_c	D_b *Predicted (mm)*	f_b *Predicted (s-1)*
0.61	0.075	0.57	5.2	18	169	152.99	0.93	5.3	20
0.61	0.1	0.58	5.3	23	225	271.97	0.91	5.5	24
0.61	0.125	0.58	5.5	26	281	424.96	0.91	5.7	27
0.61	0.15	0.59	5.6	32	338	611.94	0.90	5.8	30
0.71	0.05	0.56	5.6	10	97	43.12	0.95	5.3	13
0.71	0.075	0.56	5.7	14	145	97.02	0.95	5.5	17
0.71	0.1	0.56	5.7	18	193	172.48	0.95	5.8	20
0.71	0.125	0.56	5.9	22	242	269.50	0.95	5.9	23
0.71	0.15	0.57	6.2	25	290	388.08	0.93	6.1	26
0.81	0.05	0.56	5.6	9	85	29.04	0.95	5.5	12
0.81	0.075	0.56	5.8	13	127	65.34	0.95	5.8	15
0.81	0.1	0.56	5.8	17	170	116.16	0.95	6.1	18
0.81	0.125	0.56	5.9	20	212	181.50	0.95	6.2	20
0.81	0.15	0.56	6.3	24	254	261.36	0.95	6.4	22
0.91	0.05	0.55	5.9	7	75	20.48	0.96	5.7	10
0.91	0.075	0.55	6.1	10	113	46.08	0.96	6.1	13
0.91	0.1	0.55	6.3	13	151	81.92	0.96	6.3	16
0.91	0.125	0.55	6.5	16	189	128.00	0.96	6.5	18
0.91	0.15	0.55	6.6	18	226	184.32	0.96	6.7	20
1	0.05	0.54	6.2	7	69	15.43	0.98	5.9	9
1	0.075	0.54	6.3	9	103	34.72	0.98	6.3	12
1	0.1	0.54	6.5	11	137	61.73	0.98	6.5	14
1	0.125	0.54	6.6	13	172	96.46	0.98	6.7	16
1	0.15	0.54	6.9	15	206	138.90	0.98	6.9	18

***Static Pressure is 0.53 PSI (equivalent to around 14.7 inch of water).**

Appendix B: Aeration Efficiency Calculations

Orifice Size (mm)	Flow Rate (SLPM)	Total Pressure (KPa)	Atm Pressure (Kpa)	Temperature (°C)	Bubble Avg. size (mm)	Avg. Bubble Velocity (m/s)	Plume Size (mm)	Height (m)	Water Volume (L)	Saturated DO (mg/L)	KLa (1/h)	SOTR (Kg/h)	SAE (KgO2/KW.h)	ε_b	$\frac{p_s}{p_c}$	$\frac{A_a}{A_t}$	$\frac{h_d}{D_t}$	$\frac{D_b}{D_o}$	SAE Predicted (KgO2/KW.h)
0.41	0.05	5.31	99.08	19.7	4	0.32	42	0.4572	2.2	8.88	1.71	3.35E-05	7.56	5.41E-04	0.84	0.30	6	0.10	7.19
0.41	0.075	5.35	99.28	19.8	4.3	0.33	45	0.4572	2.2	8.88	2.13	4.15E-05	6.21	7.87E-04	0.84	0.35	6	0.10	6.16
0.41	0.1	5.38	99.22	19.6	4.7	0.36	48	0.4572	2.2	8.91	2.55	5.00E-05	5.57	9.62E-04	0.83	0.40	6	0.09	5.69
0.41	0.125	5.59	98.87	19.8	4.9	0.36	49	0.4572	2.2	8.84	2.90	5.64E-05	4.85	1.20E-03	0.80	0.41	6	0.08	5.02
0.41	0.15	5.72	98.25	19.7	5.4	0.39	50	0.4572	2.2	8.80	3.08	5.96E-05	4.17	1.33E-03	0.78	0.43	6	0.08	4.70
0.41	0.05	7.55	99.91	19.7	4	0.32	42	0.6858	3.3	8.95	1.55	4.59E-05	7.29	5.41E-04	0.89	0.30	9	0.10	7.22
0.41	0.075	7.59	99.84	19.4	4.3	0.33	45	0.6858	3.3	9.00	2.08	6.17E-05	6.50	7.87E-04	0.89	0.35	9	0.10	6.20
0.41	0.1	7.62	99.49	19.9	4.7	0.36	48	0.6858	3.3	8.88	2.56	7.50E-05	5.90	9.62E-04	0.88	0.40	9	0.09	5.73
0.41	0.125	7.83	99.42	19.3	4.9	0.36	49	0.6858	3.3	8.98	2.82	8.37E-05	5.13	1.20E-03	0.86	0.41	9	0.08	5.10
0.41	0.15	7.97	99.42	19.7	5.4	0.39	50	0.6858	3.3	8.91	3.06	9.00E-05	4.52	1.33E-03	0.84	0.43	9	0.08	4.80
0.41	0.05	9.79	99.15	19.9	4	0.32	42	0.9144	4.4	8.85	1.58	6.14E-05	7.52	5.41E-04	0.92	0.30	12	0.10	7.20
0.41	0.075	9.83	99.28	20	4.3	0.33	45	0.9144	4.4	8.84	1.91	7.43E-05	6.05	7.87E-04	0.91	0.35	12	0.10	6.18
0.41	0.1	9.86	99.08	20.3	4.7	0.36	48	0.9144	4.4	8.77	2.44	9.43E-05	5.74	9.62E-04	0.91	0.40	12	0.09	5.72
0.41	0.125	10.07	98.73	20	4.9	0.36	49	0.9144	4.4	8.79	2.78	1.07E-04	5.12	1.20E-03	0.89	0.41	12	0.08	5.12
0.41	0.15	10.21	98.32	19.7	5.4	0.39	50	0.9144	4.4	8.81	2.88	1.11E-04	4.37	1.33E-03	0.88	0.43	12	0.08	4.82
0.41	0.05	12.04	98.94	19.8	4	0.32	42	1.143	5.5	8.85	1.44	7.02E-05	6.99	5.41E-04	0.93	0.30	15	0.10	7.15
0.41	0.075	12.07	99.01	20.1	4.3	0.33	45	1.143	5.5	8.80	1.97	9.54E-05	6.32	7.87E-04	0.93	0.35	15	0.10	6.15
0.41	0.1	12.11	99.15	20.2	4.7	0.36	48	1.143	5.5	8.79	2.01	9.71E-05	4.81	9.62E-04	0.93	0.40	15	0.09	5.69
0.41	0.125	12.31	99.15	19.6	4.9	0.36	49	1.143	5.5	8.90	2.79	1.37E-04	5.32	1.20E-03	0.91	0.41	15	0.08	5.10
0.41	0.15	12.45	99.28	19.7	5.4	0.39	50	1.143	5.5	8.90	2.99	1.46E-04	4.70	1.33E-03	0.90	0.43	15	0.08	4.82
0.41	0.05	14.28	99.15	20.1	4	0.32	42	1.3716	6.6	8.81	1.31	7.64E-05	6.42	5.41E-04	0.94	0.30	18	0.10	7.10

Orifice Size (mm)	Flow Rate (SLPM)	Total Pressure (KPa)	Atm Pressure (Kpa)	Temperature (°C)	Bubble Avg. size (mm)	Avg. Bubble Velocity (m/s)	Plume Size (mm)	Height (m)	Water Volume (L)	Saturated DO (mg/L)	KLa (1/h)	SOTR (Kg/h)	SAE (KgO2/KW.h)	ε_b	$\frac{p_s}{p_c}$	$\frac{A_a}{A_t}$	$\frac{h_d}{D_t}$	$\frac{D_b}{D_o}$	SAE Predicted (KgO2/KW.h)
0.41	0.075	14.31	99.35	20.1	4.3	0.33	45	1.3716	6.6	8.83	2.09	1.22E-04	6.80	7.87E-04	0.94	0.35	18	0.10	6.11
0.41	0.1	14.35	99.35	20.1	4.7	0.36	48	1.3716	6.6	8.83	2.42	1.41E-04	5.89	9.62E-04	0.94	0.40	18	0.09	5.66
0.41	0.125	14.55	98.94	20	4.9	0.36	49	1.3716	6.6	8.81	2.65	1.54E-04	5.08	1.20E-03	0.92	0.41	18	0.08	5.08
0.41	0.15	14.69	98.46	20	5.4	0.39	50	1.3716	6.6	8.77	3.03	1.75E-04	4.77	1.33E-03	0.92	0.43	18	0.08	4.80
0.34	0.05	5.38	98.25	19	3.9	0.31	47	0.4572	2.2	8.93	1.74	3.43E-05	7.64	5.59E-04	0.83	0.38	6	0.09	7.20
0.34	0.075	5.45	98.04	20.3	4.5	0.33	49	0.4572	2.2	8.68	2.39	4.56E-05	6.69	7.87E-04	0.82	0.41	6	0.08	6.11
0.34	0.1	5.66	98.18	19.6	4.7	0.36	50	0.4572	2.2	8.82	2.91	5.65E-05	5.99	9.62E-04	0.79	0.43	6	0.07	5.45
0.34	0.125	5.93	97.91	20	5.2	0.34	51	0.4572	2.2	8.72	3.49	6.70E-05	5.42	1.27E-03	0.76	0.45	6	0.07	4.62
0.34	0.15	6.14	98.04	20	5.4	0.36	52	0.4572	2.2	8.73	4.06	7.80E-05	5.08	1.44E-03	0.73	0.47	6	0.06	4.28
0.34	0.05	7.62	99.56	19.8	3.9	0.31	47	0.6858	3.3	8.90	1.57	4.60E-05	7.24	5.59E-04	0.88	0.38	9	0.09	7.25
0.34	0.075	7.69	99.28	19.6	4.5	0.33	49	0.6858	3.3	8.92	2.10	6.19E-05	6.43	7.87E-04	0.87	0.41	9	0.08	6.17
0.34	0.1	7.90	99.22	20	4.7	0.36	50	0.6858	3.3	8.84	2.45	7.16E-05	5.43	9.62E-04	0.85	0.43	9	0.07	5.55
0.34	0.125	8.17	99.49	19.7	5.2	0.34	51	0.6858	3.3	8.92	2.75	8.09E-05	4.75	1.27E-03	0.82	0.45	9	0.07	4.75
0.34	0.15	8.38	99.56	19.5	5.4	0.36	52	0.6858	3.3	8.96	3.08	9.10E-05	4.34	1.44E-03	0.80	0.47	9	0.06	4.43
0.34	0.05	9.86	98.11	19.7	3.9	0.31	47	0.9144	4.4	8.79	1.48	5.72E-05	6.95	5.59E-04	0.91	0.38	12	0.09	7.24
0.34	0.075	9.93	98.11	20	4.5	0.33	49	0.9144	4.4	8.74	1.99	7.65E-05	6.16	7.87E-04	0.90	0.41	12	0.08	6.17
0.34	0.1	10.14	97.77	20	4.7	0.36	50	0.9144	4.4	8.71	2.32	8.88E-05	5.25	9.62E-04	0.88	0.43	12	0.07	5.57
0.34	0.125	10.41	98.04	20	5.2	0.34	51	0.9144	4.4	8.73	2.58	9.92E-05	4.57	1.27E-03	0.86	0.45	12	0.07	4.80
0.34	0.15	10.62	98.18	20	5.4	0.36	52	0.9144	4.4	8.74	2.91	1.12E-04	4.22	1.44E-03	0.84	0.47	12	0.06	4.49
0.34	0.05	12.11	97.63	20	3.9	0.31	47	1.143	5.5	8.70	1.42	6.80E-05	6.73	5.59E-04	0.93	0.38	15	0.09	7.20
0.34	0.075	12.17	97.49	20	4.5	0.33	49	1.143	5.5	8.68	1.84	8.80E-05	5.78	7.87E-04	0.92	0.41	15	0.08	6.14
0.34	0.1	12.38	97.42	20.3	4.7	0.36	50	1.143	5.5	8.62	2.33	1.10E-04	5.34	9.62E-04	0.91	0.43	15	0.07	5.56
0.34	0.125	12.66	97.42	19.7	5.2	0.34	51	1.143	5.5	8.73	2.61	1.25E-04	4.75	1.27E-03	0.89	0.45	15	0.07	4.81

Orifice Size (mm)	Flow Rate (SLPM)	Total Pressure (KPa)	Atm Pressure (Kpa)	Temperature (°C)	Bubble Avg. size (mm)	Avg. Bubble Velocity (m/s)	Plume Size (mm)	Height (m)	Water Volume (L)	Saturated DO (mg/L)	KLa (1/h)	SOTR (Kg/h)	SAE (KgO2/KW.h)	ε_b	$\frac{p_s}{p_c}$	$\frac{A_a}{A_t}$	$\frac{h_d}{D_t}$	$\frac{D_b}{D_o}$	SAE Predicted (KgO2/KW.h)
0.34	0.15	12.86	97.42	19.5	5.4	0.36	52	1.143	5.5	8.77	3.13	1.51E-04	4.69	1.44E-03	0.87	0.47	15	0.06	4.51
0.34	0.05	14.35	98.11	20	3.9	0.31	47	1.3716	6.6	8.74	1.42	8.18E-05	6.84	5.59E-04	0.94	0.38	18	0.09	7.16
0.34	0.075	14.42	97.70	20	4.5	0.33	49	1.3716	6.6	8.70	1.83	1.05E-04	5.84	7.87E-04	0.93	0.41	18	0.08	6.11
0.34	0.1	14.62	97.77	19.7	4.7	0.36	50	1.3716	6.6	8.76	2.25	1.30E-04	5.34	9.62E-04	0.92	0.43	18	0.07	5.54
0.34	0.125	14.90	97.84	20	5.2	0.34	51	1.3716	6.6	8.71	2.60	1.49E-04	4.81	1.27E-03	0.90	0.45	18	0.07	4.80
0.34	0.15	15.11	97.15	20.4	5.4	0.36	52	1.3716	6.6	8.58	2.74	1.55E-04	4.11	1.44E-03	0.89	0.47	18	0.06	4.51
0.3	0.05	5.38	98.94	19.4	3.9	0.32	49	0.4572	2.2	8.92	1.66	3.25E-05	7.26	5.41E-04	0.83	0.41	6	0.08	7.31
0.3	0.075	5.66	98.87	20.4	4.2	0.35	51	0.4572	2.2	8.73	2.12	4.06E-05	5.75	7.42E-04	0.79	0.45	6	0.07	6.16
0.3	0.1	6.35	97.29	19.9	4.6	0.37	53	0.4572	2.2	8.68	2.62	5.00E-05	4.73	9.36E-04	0.71	0.48	6	0.07	5.13
0.3	0.125	6.76	97.08	20.5	4.8	0.38	54	0.4572	2.2	8.56	2.98	5.60E-05	3.98	1.14E-03	0.66	0.50	6	0.06	4.50
0.3	0.15	7.52	97.08	19.7	5	0.38	55	0.4572	2.2	8.70	3.54	6.77E-05	3.60	1.37E-03	0.60	0.52	6	0.06	3.85
0.3	0.05	7.59	99.63	19.8	3.9	0.32	49	0.6858	3.3	8.91	1.69	4.96E-05	7.84	5.41E-04	0.89	0.41	9	0.08	7.39
0.3	0.075	8.21	97.15	19.7	4.2	0.35	51	0.6858	3.3	8.71	2.15	6.18E-05	6.02	7.42E-04	0.82	0.45	9	0.07	6.11
0.3	0.1	8.48	97.22	20	4.6	0.37	53	0.6858	3.3	8.66	2.53	7.24E-05	5.12	9.36E-04	0.79	0.48	9	0.07	5.39
0.3	0.125	8.83	99.63	19.6	4.8	0.38	54	0.6858	3.3	8.95	2.87	8.46E-05	4.60	1.14E-03	0.76	0.50	9	0.06	4.81
0.3	0.15	9.59	99.63	19.9	5	0.38	55	0.6858	3.3	8.89	3.40	9.98E-05	4.16	1.37E-03	0.70	0.52	9	0.06	4.19
0.3	0.05	10.00	98.87	20.3	3.9	0.32	49	0.9144	4.4	8.75	1.71	6.59E-05	7.91	5.41E-04	0.90	0.41	12	0.08	7.28
0.3	0.075	10.28	97.15	20.4	4.2	0.35	51	0.9144	4.4	8.58	2.23	8.44E-05	6.56	7.42E-04	0.87	0.45	12	0.07	6.24
0.3	0.1	10.76	98.87	20.4	4.6	0.37	53	0.9144	4.4	8.73	2.54	9.75E-05	5.43	9.36E-04	0.83	0.48	12	0.07	5.46
0.3	0.125	11.31	97.22	20.4	4.8	0.38	54	0.9144	4.4	8.59	2.91	1.10E-04	4.66	1.14E-03	0.79	0.50	12	0.06	4.84
0.3	0.15	11.86	97.08	20	5	0.38	55	0.9144	4.4	8.65	3.40	1.29E-04	4.36	1.37E-03	0.76	0.52	12	0.06	4.32
0.3	0.05	12.14	99.97	19.7	3.9	0.32	49	1.143	5.5	8.96	1.56	7.67E-05	7.58	5.41E-04	0.92	0.41	15	0.08	7.30
0.3	0.075	12.62	99.15	19.8	4.2	0.35	51	1.143	5.5	8.87	2.24	1.09E-04	6.93	7.42E-04	0.89	0.45	15	0.07	6.20

Orifice Size (mm)	Flow Rate (SLPM)	Total Pressure (KPa)	Atm Pressure (Kpa)	Temperature (°C)	Bubble Avg. size (mm)	Avg. Bubble Velocity (m/s)	Plume Size (mm)	Height (m)	Water Volume (L)	Saturated DO (mg/L)	KLa (1/h)	SOTR (Kg/h)	SAE (KgO2/KW.h)	ε_b	$\frac{p_s}{p_c}$	$\frac{A_a}{A_t}$	$\frac{h_d}{D_t}$	$\frac{D_b}{D_o}$	SAE Predicted (KgO2/KW.h)
0.3	0.1	12.69	98.80	20.1	4.6	0.37	53	1.143	5.5	8.78	2.56	1.24E-04	5.85	9.36E-04	0.88	0.48	15	0.07	5.59
0.3	0.125	13.59	99.35	20	4.8	0.38	54	1.143	5.5	8.85	3.02	1.47E-04	5.18	1.14E-03	0.82	0.50	15	0.06	4.89
0.3	0.15	14.07	99.49	19.7	5	0.38	55	1.143	5.5	8.92	3.40	1.66E-04	4.73	1.37E-03	0.80	0.52	15	0.06	4.40
0.3	0.05	14.35	100.04	20.3	3.9	0.32	49	1.3716	6.6	8.86	1.66	9.71E-05	8.11	5.41E-04	0.94	0.41	18	0.08	7.27
0.3	0.075	14.83	100.04	19.7	4.2	0.35	51	1.3716	6.6	8.96	2.17	1.29E-04	6.93	7.42E-04	0.91	0.45	18	0.07	6.20
0.3	0.1	15.11	99.97	20.3	4.6	0.37	53	1.3716	6.6	8.85	2.30	1.34E-04	5.32	9.36E-04	0.89	0.48	18	0.07	5.54
0.3	0.125	15.59	99.97	19.7	4.8	0.38	54	1.3716	6.6	8.96	2.39	1.41E-04	4.35	1.14E-03	0.86	0.50	18	0.06	4.97
0.3	0.15	16.21	99.56	19.8	5	0.38	55	1.3716	6.6	8.90	3.40	2.00E-04	4.93	1.37E-03	0.83	0.52	18	0.06	4.46
0.25	0.05	5.93	99.15	19.8	3.8	0.33	50	0.4572	2.2	8.87	1.59	3.11E-05	6.28	5.25E-04	0.76	0.43	6	0.07	6.83
0.25	0.075	6.62	100.04	19.7	4.1	0.34	52	0.4572	2.2	8.96	2.28	4.50E-05	5.43	7.64E-04	0.68	0.47	6	0.06	5.37
0.25	0.1	7.59	100.11	20	4.5	0.36	54	0.4572	2.2	8.92	2.66	5.21E-05	4.12	9.62E-04	0.59	0.50	6	0.06	4.40
0.25	0.125	9.03	99.15	19.6	4.6	0.36	55	0.4572	2.2	8.90	3.35	6.56E-05	3.48	1.20E-03	0.50	0.52	6	0.05	3.53
0.25	0.15	10.55	99.22	20.7	4.8	0.36	56	0.4572	2.2	8.71	4.00	7.66E-05	2.90	1.44E-03	0.42	0.54	6	0.05	2.91
0.25	0.05	10.24	99.84	19.5	3.8	0.33	50	0.6858	3.3	8.98	1.67	4.96E-05	5.81	5.25E-04	0.66	0.43	9	0.07	5.97
0.25	0.075	10.93	99.77	20.4	4.1	0.34	52	0.6858	3.3	8.81	2.23	6.50E-05	4.75	7.64E-04	0.62	0.47	9	0.06	4.84
0.25	0.1	12.17	99.91	19.9	4.5	0.36	54	0.6858	3.3	8.92	2.68	7.89E-05	3.89	9.62E-04	0.55	0.50	9	0.06	4.06
0.25	0.125	13.28	99.91	19.6	4.6	0.36	55	0.6858	3.3	8.97	3.10	9.18E-05	3.32	1.20E-03	0.51	0.52	9	0.05	3.46
0.25	0.15	14.79	99.91	20.3	4.8	0.36	56	0.6858	3.3	8.84	3.69	1.08E-04	2.91	1.44E-03	0.45	0.54	9	0.05	2.96
0.25	0.05	14.76	100.11	19.8	3.8	0.33	50	0.9144	4.4	8.95	1.47	5.77E-05	4.69	5.25E-04	0.61	0.43	12	0.07	5.51
0.25	0.075	15.72	99.97	19.9	4.1	0.34	52	0.9144	4.4	8.92	1.92	7.56E-05	3.84	7.64E-04	0.57	0.47	12	0.06	4.48
0.25	0.1	16.55	99.22	20.4	4.5	0.36	54	0.9144	4.4	8.76	2.59	9.98E-05	3.62	9.62E-04	0.54	0.50	12	0.06	3.91
0.25	0.125	17.86	99.15	19.8	4.6	0.36	55	0.9144	4.4	8.87	3.18	1.24E-04	3.33	1.20E-03	0.50	0.52	12	0.05	3.36
0.25	0.15	19.10	99.15	19.8	4.8	0.36	56	0.9144	4.4	8.87	3.75	1.46E-04	3.06	1.44E-03	0.47	0.54	12	0.05	2.96

Orifice Size (mm)	Flow Rate (SLPM)	Total Pressure (KPa)	Atm Pressure (Kpa)	Temperature (°C)	Bubble Avg. size (mm)	Avg. Bubble Velocity (m/s)	Plume Size (mm)	Height (m)	Water Volume (L)	Saturated DO (mg/L)	KLa (1/h)	SOTR (Kg/h)	SAE (KgO2/KW.h)	ε_b	$\frac{p_s}{p_c}$	$\frac{A_a}{A_t}$	$\frac{h_d}{D_t}$	$\frac{D_b}{D_o}$	SAE Predicted (KgO2/KW.h)
0.25	0.05	19.28	99.42	19.7	3.8	0.33	50	1.143	5.5	8.91	1.49	7.32E-05	4.55	5.25E-04	0.58	0.43	15	0.07	5.25
0.25	0.075	20.03	99.15	19.6	4.1	0.34	52	1.143	5.5	8.90	2.27	1.11E-04	4.44	7.64E-04	0.56	0.47	15	0.06	4.34
0.25	0.1	21.07	99.22	19.6	4.5	0.36	54	1.143	5.5	8.91	2.20	1.08E-04	3.07	9.62E-04	0.53	0.50	15	0.06	3.79
0.25	0.125	22.24	99.15	19.8	4.6	0.36	55	1.143	5.5	8.87	3.16	1.54E-04	3.33	1.20E-03	0.50	0.52	15	0.05	3.31
0.25	0.15	23.41	99.56	19.6	4.8	0.36	56	1.143	5.5	8.94	3.68	1.81E-04	3.09	1.44E-03	0.48	0.54	15	0.05	2.95
0.25	0.05	23.72	100.59	19.5	3.8	0.33	50	1.3716	6.6	9.05	1.63	9.73E-05	4.92	5.25E-04	0.57	0.43	18	0.07	5.07
0.25	0.075	24.14	100.73	20.2	4.1	0.34	52	1.3716	6.6	8.93	2.25	1.33E-04	4.39	7.64E-04	0.56	0.47	18	0.06	4.26
0.25	0.1	25.17	99.56	20.4	4.5	0.36	54	1.3716	6.6	8.80	2.72	1.58E-04	3.75	9.62E-04	0.53	0.50	18	0.06	3.74
0.25	0.125	26.28	100.80	19.4	4.6	0.36	55	1.3716	6.6	9.09	3.33	2.00E-04	3.64	1.20E-03	0.51	0.52	18	0.05	3.30
0.25	0.15	27.72	100.53	19.4	4.8	0.36	56	1.3716	6.6	9.06	4.06	2.43E-04	3.50	1.44E-03	0.49	0.54	18	0.05	2.93
0.2	0.05	8.07	99.35	19.5	3.7	0.33	52	0.4572	2.2	8.94	1.94	3.81E-05	5.67	5.25E-04	0.56	0.47	6	0.05	5.43
0.2	0.076	10.96	99.42	19.8	4	0.35	54	0.4572	2.2	8.89	2.55	4.99E-05	3.59	7.52E-04	0.41	0.50	6	0.05	3.72
0.2	0.099	14.34	98.46	19.5	4.4	0.35	56	0.4572	2.2	8.86	3.26	6.35E-05	2.68	9.80E-04	0.31	0.54	6	0.05	2.73
0.2	0.125	18.82	98.46	19.9	4.7	0.35	57	0.4572	2.2	8.79	4.04	7.82E-05	1.99	1.24E-03	0.24	0.56	6	0.04	2.02
0.2	0.15	23.93	98.60	20.3	4.2	0.37	58	0.4572	2.2	8.73	5.16	9.91E-05	1.66	1.40E-03	0.19	0.58	6	0.05	1.64
0.2	0.05	12.31	97.22	19.7	3.7	0.33	52	0.6858	3.3	8.71	1.81	5.22E-05	5.08	5.25E-04	0.55	0.47	9	0.05	5.19
0.2	0.074	15.21	97.15	19.7	4	0.35	54	0.6858	3.3	8.71	2.43	6.98E-05	3.72	7.32E-04	0.44	0.50	9	0.05	3.86
0.2	0.1	18.79	97.15	19.4	4.4	0.35	56	0.6858	3.3	8.76	3.26	9.42E-05	3.01	9.90E-04	0.36	0.54	9	0.05	2.90
0.2	0.125	23.07	97.08	19.5	4.7	0.35	57	0.6858	3.3	8.73	3.97	1.15E-04	2.38	1.24E-03	0.29	0.56	9	0.04	2.26
0.2	0.151	27.82	97.08	20	4.2	0.37	58	0.6858	3.3	8.65	5.16	1.47E-04	2.10	1.41E-03	0.24	0.58	9	0.05	1.90
0.2	0.05	16.76	99.35	19.6	3.7	0.33	52	0.9144	4.4	8.92	1.82	7.13E-05	5.10	5.25E-04	0.54	0.47	12	0.05	4.99
0.2	0.075	19.58	99.42	20.2	4	0.35	54	0.9144	4.4	8.82	2.47	9.60E-05	3.92	7.42E-04	0.46	0.50	12	0.05	3.84
0.2	0.1	22.96	98.53	19.7	4.4	0.35	56	0.9144	4.4	8.83	3.22	1.25E-04	3.26	9.90E-04	0.39	0.54	12	0.05	3.02

Orifice Size (mm)	Flow Rate (SLPM)	Total Pressure (KPa)	Atm Pressure (Kpa)	Temperature (°C)	Bubble Avg. size (mm)	Avg. Bubble Velocity (m/s)	Plume Size (mm)	Height (m)	Water Volume (L)	Saturated DO (mg/L)	KLa (1/h)	SOTR (Kg/h)	SAE (KgO2/KW.h)	ε_b	$\frac{p_s}{p_c}$	$\frac{A_a}{A_t}$	$\frac{h_d}{D_t}$	$\frac{D_b}{D_o}$	SAE Predicted (KgO2/KW.h)
0.2	0.125	27.03	98.46	19.8	4.7	0.35	57	0.9144	4.4	8.80	4.07	1.58E-04	2.80	1.24E-03	0.33	0.56	12	0.04	2.42
0.2	0.151	32.27	98.53	20	4.2	0.37	58	0.9144	4.4	8.77	5.57	2.15E-04	2.65	1.41E-03	0.28	0.58	12	0.05	2.05
0.2	0.049	25.65	99.35	20	3.7	0.33	52	1.3716	6.6	8.85	1.70	9.91E-05	4.73	5.14E-04	0.52	0.47	18	0.05	4.80
0.2	0.074	28.14	99.56	19.8	4	0.35	54	1.3716	6.6	8.90	2.38	1.40E-04	4.03	7.32E-04	0.48	0.50	18	0.05	3.85
0.2	0.099	31.38	99.70	19.5	4.4	0.35	56	1.3716	6.6	8.97	2.92	1.73E-04	3.34	9.80E-04	0.43	0.54	18	0.05	3.13
0.2	0.125	35.51	99.84	19.7	4.7	0.35	57	1.3716	6.6	8.95	4.04	2.39E-04	3.22	1.24E-03	0.38	0.56	18	0.04	2.58
0.2	0.15	48.75	100.46	19.7	4.2	0.37	58	1.3716	6.6	9.00	4.80	2.85E-04	2.34	1.40E-03	0.28	0.58	18	0.05	1.98